INTERFACE FOCUS

rsfs.royalsocietypublishing.org

Research

Cite this article: Oyston JW, Hughes M, Wagner PJ, Gerber S, Wills MA. 2015 What limits the morphological disparity of clades? *Interface Focus* **5**: 20150042.
http://dx.doi.org/10.1098/rsfs.2015.0042

One contribution of 12 to a theme issue 'Are there limits to evolution?'

Subject Areas:
biocomplexity

Keywords:
morphological disparity, homoplasy, character states, bodyplan, developmental constraints, ecological restrictions

Author for correspondence:
Matthew A. Wills
e-mail: m.a.wills@bath.ac.uk

What limits the morphological disparity of clades?

Jack W. Oyston[1], Martin Hughes[2], Peter J. Wagner[3], Sylvain Gerber[4] and Matthew A. Wills[1]

[1]The Milner Centre for Evolution, Department of Biology & Biochemistry, University of Bath, Bath BA2 7AY, UK
[2]Department of Life Sciences, The Natural History Museum, London SW7 5BD, UK
[3]Department of Paleobiology, National Museum of Natural History, Smithsonian Institution, Washington, DC 20013-7012, USA
[4]Department of Earth Sciences, University of Cambridge, Cambridge CB2 3EQ, UK

The morphological disparity of species within major clades shows a variety of trajectory patterns through evolutionary time. However, there is a significant tendency for groups to reach their maximum disparity relatively early in their histories, even while their species richness or diversity is comparatively low. This pattern of early high-disparity suggests that there are internal constraints (e.g. developmental pleiotropy) or external restrictions (e.g. ecological competition) upon the variety of morphologies that can subsequently evolve. It has also been demonstrated that the rate of evolution of new character states decreases in most clades through time (character saturation), as does the rate of origination of novel bodyplans and higher taxa. Here, we tested whether there was a simple relationship between the level or rate of character state exhaustion and the shape of a clade's disparity profile: specifically, its centre of gravity (CG). In a sample of 93 extinct major clades, most showed some degree of exhaustion, but all continued to evolve new states up until their extinction. Projection of states/steps curves suggested that clades realized an average of 60% of their inferred maximum numbers of states. Despite a weak but significant correlation between overall levels of homoplasy and the CG of clade disparity profiles, there were no significant relationships between any of our indices of exhaustion curve shape and the clade disparity CG. Clades showing early high-disparity were no more likely to have early character saturation than those with maximum disparity late in their evolution.

1. Introduction

Much like the species and individuals that constitute them, all clades have an origin and all must ultimately suffer extinction. Their intervening histories, however, can follow a variety of complex trajectories. The study of these patterns is central to the study of macroevolution, with questions centring on whether there is a typical pattern [1–7], whether the fortunes of clades are positively or negatively correlated [8–13] and whether there are particular responses to marked environmental changes [14]. Clade evolution is commonly studied by plotting diversity (numbers of constituent species, genera or higher taxa) through time, which can highlight periods of elevated diversification, extinction and turnover, as well as potential interactions between groups [15–20]. All Phanerozoic diversity curves affirm some form of increasing trajectory, variously modified by physical and biological factors [21]. Diversity change within individual clades can be modelled using relatively simple birth/death processes with constant parameters [22], which predict symmetrical clade shapes—waxing and waning diversity through time—as a null. More complex and asymmetrical patterns result from models in which parameters are varied through time [6,23,24]. Gould *et al.* [25] summarized the evolutionary trajectories for extinct clades using a simple measure of their centre of gravity (CG), with a symmetrical clade trajectory having a CG of 0.5. Empirical studies revealed a tendency towards bottom-heaviness (CG < 0.5), with clades typically reaching their highest diversity relatively early in their evolution.

THE ROYAL SOCIETY PUBLISHING

1.1. What is disparity?

In addition to assessments of diversity, it is increasingly common to investigate the morphological variety or disparity of clades through time (see summaries in Erwin [26] and Wagner [6]). All indices of disparity are relative and depend upon the nature of variables used to quantify form and the manner in which these variables are summarized [27]. Most use some form of morphospace; a multidimensional space-filling plot in which the distances between taxa are proportional to the measured morphological differences between them [28]. These may themselves be visualized using data reduction and ordination techniques (e.g. principal components or coordinates) to summarize variation in the original set of morphological variables within a smaller number of abstracted axes. Several indices of disparity assess the distribution of taxa in such morphospaces: for example, by adding the ranges or variances on successive axes (a boxing approach), using convex hulls or determining the mean distance between all pairs of taxa. Indices can then be used to compare the disparity of constituent subclades, or to track the morphospace occupation of one or more groups through time, thereby building up a disparity profile [6,28–32]. When multiple disparity indices are used to capture variation in the same aspects of form, these often show a high degree of congruence. However, conflicting patterns are possible, depending upon the variance structure of the data [28–32].

Counterintuitively, diversity and disparity appear to be fundamentally decoupled [6]. Some periods or clades contain modest numbers of species that are nevertheless highly distinct morphologically, whereas others contain much greater numbers of morphologically very conservative species. More broadly, some of the most speciose groups (e.g. beetles and insects more generally) have some of the most constrained bodyplans; indeed, there are suggestions that a constrained and entrenched bodyplan might even be conducive to higher diversity [33]. Because clades evolve by lineage branching, we would expect a progressive exploration of morphospace even via a random walk. Once occupied, however, random extinction processes will tend to winnow out the space, but are less likely to leave large regions entirely vacant. All other things being equal, therefore, clades might be expected to have top-heavy disparity profiles through time, although driven evolutionary trends and selective extinction patterns may easily combine to yield a diversity of profile shapes. Empirical investigations for major clades over the past 25 years also show many different patterns, but the most common counterintuitively entails comparatively high-disparity relatively early in the clade's history (see also simulations by Foote [24,34,35]). Many groups therefore appear to explore the range of available 'design' options quite quickly, with subsequent evolution principally serving to increase diversity, possibly by the progressively fine subdivision of niche space [7,26,36].

1.2. Why might clades show early high-disparity?

One possible explanation for early high-disparity is that there are constraints and restrictions upon the available morphospace, thereby limiting the potential for expansion [37–40]. Once filled, the space can only be subdivided or vacated unless the constraints are removed or a clade evolves so as to circumvent them [41]. Such limits can be broadly classified in four categories: geometric, ontogenetic, physical and environmental.

Geometric constraints are those that can be predicted for any form in any context (many shapes are geometrically impossible), and are not limited to biological structures. Additional limits are imposed by particular generative processes [42] such that ontogeny can sometimes also be modelled geometrically. In such cases, it may be possible to delimit a morphospace theoretically [43], subsequently plotting real specimens within this. The best-known example is the shell of molluscs [44]. All forms—from simple cones (e.g. belemnites, patelloid limpets and hyolithids) to planispiral coils (e.g. many ammonites and bivalves) and translated coils (e.g. most gastropods)—can be modelled with reference to three or fewer variables that describe growth patterns, defining the theoretical morphospace. Forms outside of this are geometrically and ontogenetically impossible; typically, because the shell cannot grow through itself. However, many regions of the theoretical space are never occupied [42]. Actualized morphologies are limited to a relatively small fraction of the space, despite the half-billion-year history of molluscs, during which time groups have repeatedly re-radiated in the wake of mass extinctions, and within which there is rampant convergence in gross form [45–47]. Additional limits must apply, therefore. There are more ontogenetic constraints upon form than those predictable geometrically. Organisms develop by the complex interplay of mutually inductive systems and feedback loops, themselves underpinned by cascades of genetic control: not all developmental trajectories and morphologies are possible [48]. Further limits to the evolution of disparity are physical, but understanding these requires additional knowledge of biological context. Form is limited by the properties of biological materials, but the performance of such materials depends upon the function of the structures that they compose, and the context and environment in which they are deployed. For example, the physical constraints upon walking [49–52] and swimming [53,54] vertebrates differ from an engineering standpoint. Environmental restrictions [6] can therefore be both physical and biological, and might be broadly defined as all those factors that determine the availability of ecospace or niche space. A lineage can only evolve to realize a particular morphology if there are selective advantages; not only to the endpoint, but also to all intermediate forms along that evolutionary trajectory. The physical and biological environments are also dynamic and coupled systems.

1.3. Can we detect the operation of limits on disparity from levels and patterns of homoplasy?

If a clade has evolved to explore the limits of its morphospace, then its constituent lineages (variously prevented from exploring novel morphologies) might be more constrained or restricted to revisit previously occupied regions. This could be realized as increased levels of character state reversal and convergence. Overall levels of homoplasy might therefore be expected to be higher in constrained clades than in those free to colonize new regions of their morphospace. Most indices of homoplasy are influenced by dataset dimensions [55], but the homoplasy excess ratio (HER) of Archie [56] is a relatively unbiased ensemble metric that can be compared across clades [57]. The commonly reported ensemble consistency index is simply the ratio of the minimum possible number of steps (i.e. the number of derived states; MINL) to the number of steps observed on the optimal tree(s) (L). By comparison, the HER includes a term for the mean number of steps in optimal

trees inferred from randomized data (MEANNS); specifically, a large number of matrices in which the assignment of states has been randomized within characters but across taxa. The HER is then given by

$$\mathrm{HER} = 1.0 - \frac{\mathrm{L} - \mathrm{MINL}}{\mathrm{MEANNS} - \mathrm{MINL}}.$$

Nonetheless, overall levels of homoplasy may be less informative than the trajectory with which homoplastic changes are accrued in transitioning from the root to the terminals of a phylogeny. Wagner [58] noted that the rate of novel character state evolution usually decreased over the lifetime of a clade [59,60], with some groups approaching an asymptote and therefore character state exhaustion. If the disparity profile of clades were shaped by such exhaustion patterns, then we might expect clades reaching the bounds of their morphospaces early in their evolution (early high-disparity and low CG) to approach an earlier asymptote in numbers of realized states (character state saturation). We therefore test for such relationships here.

2. Methods

2.1. Indices of disparity

A comprehensive discussion of methods, in addition to a presentation of discrete character morphospaces, disparity profiles and summary statistics is given in Hughes *et al.* [7]. A brief summary is provided here. Our 93 discrete character matrices for metazoan clades were all sampled uniformly with respect to higher taxonomy, or were edited (by generating composite taxa) in order to standardize coverage [7]. For each clade, intertaxon distance matrices were calculated using the generalized Euclidean distance metric of Wills [32]. These matrices were ordinated in R (v. 3.0.1) [61] using principal coordinates analysis [36] and implementing Caillez's [62] correction for negative eigenvectors. Stratigraphic ranges for each constituent taxon were assigned to stages as defined in the International Stratigraphic Chart 2009 [63,64], whereas stratigraphic range data were sourced from *Sepkoski Online* [65], the *Fossil Record 2* [66] and the *Paleobiology Database* [67]. Our index of disparity was calculated as the sum of variances on all principal coordinate axes (a maximum of $n-1$ coordinates, where n is the number of sampled taxa), with the trajectory of disparity through subsequent time bins yielding a profile through time. A centre of gravity metric [25,68] in absolute time (CG_m) was calculated for each profile as

$$\mathrm{CG}_m = \frac{\Sigma d_i t_i}{\Sigma d_i}$$

where d_i is the disparity at the ith stratigraphic interval and t_i the temporal midpoint in absolute time (Myr) of the ith stratigraphic interval. This was subsequently scaled between the ages of the oldest (t_{oldest}) and youngest (t_{youngest}) intervals to yield an index of observed CG ($\mathrm{CG}_{\mathrm{scaled}}$) between 0 and 1.

$$\mathrm{CG}_{\mathrm{scaled}} = \frac{t_{\mathrm{oldest}} - \mathrm{CG}_m}{t_{\mathrm{oldest}} - t_{\mathrm{youngest}}}.$$

A clade with uniform disparity through time is highly unlikely to have a $\mathrm{CG}_{\mathrm{scaled}}$ of 0.50. Rather, the null $\mathrm{CG}_{\mathrm{scaled}}$ is determined by the durations of the time bins constituting the profile. The observed $\mathrm{CG}_{\mathrm{scaled}}$ was therefore scaled relative to the inherent CG (CG_i) for a clade of constant disparity spanning the same intervals. A bootstrap resampling procedure was used to generate a distribution of 1000 differences between $\mathrm{CG}_{\mathrm{scaled}}$ and CG_i. Clades for which more than 97.5% of these replicates lay either above or below the CG inherent in the timescale ($p < 0.05$) were deemed to be significantly top or bottom heavy, respectively [23]. Observed $\mathrm{CG}_{\mathrm{scaled}}$ was ultimately expressed relative to CG_i as a baseline, hereafter, simply CG.

We also implemented tests for early high and late high-disparity; specifically using a bootstrapping approach to determine if the disparity observed in the first or last two stages could be distinguished from the maximum level attained by the group. The 93 study clades were thereby classified as showing early or late high-disparity, and we tested for differences in our indices of homoplasy and character state saturation in these categories using Mann–Whitney *U*-tests.

A simple index of the extent to which a clade was constrained within its morphospace was derived by expressing the maximum intertaxon Euclidean distance within any time bin as a fraction of the maximum distance across all time bins. Clades closest to this maximum might also be expected to show higher levels of overall homoplasy and state saturation [7].

Finally, we also derived an index of the degree to which a clade migrated throughout its morphospace during the course of its evolution, because constant levels of disparity through time need not necessarily imply the static occupation of morphospace. We modified the D_{morpho} index of Huang *et al.* [69] to provide an index (D_{centroid}) of the degree to which the centroid of sampled taxa migrates throughout the morphospace throughout the history of the clade. For each time bin, the mean scores of the sampled taxa on each principal coordinate axis were calculated, defining the group centroid. The difference between the positions of the centroid in successive time bins on a given axis was standardized by dividing it by the full range of values realized by all taxa in all time bins. These standardized univariate distances were then used to calculate Euclidean distances between the centroid positions in successive time bins (univariate standardized distances were squared, summed and the total square rooted). Finally, the distances between all successive time bins were summed ($n-1$ comparisons for n time bins; the first time bin being a reference). Where time-series data were missing, the centroid was assumed to have remained stationary from the preceding bin.

2.2. Phylogenies and indices of homoplasy

A single outgroup taxon was used to infer ancestral character states at the base of each focal ingroup clade. Phylogenies were inferred in the program 'Tree analysis using New Technology' (TNT) [70] using Xmult level = 10, which performs a random sectorial search combined with ratchet, drift and tree fusing, followed by TBR branch swapping. The resulting most parsimonious trees (MPTs) sometimes differed from those in the source publications, especially where the taxon sample had been reduced. In cases where multiple MPTs were obtained, we selected the tree most congruent with that presented in the original publication. The character exhaustion analysis required fully resolved (dichotomously branching) trees, so polytomies were resolved stratigraphically (branching in a pectinate sequence matching their order of first fossil occurrences). It has been demonstrated that the precise trees used in character exhaustion analyses have relatively minor effects upon the results [58]. Moreover, using incorrect MPTs introduces a conservative bias because they minimize the number of steps required to achieve the observed number of character states; longer trees (even if more accurate) necessarily imply greater exhaustion by implying that greater 'sampling' of character space fails to yield additional novel states. Overall homoplasy levels were assessed using the HER of Archie [56], an index that is relatively insensitive to differences in data matrix dimensions. Five hundred randomly permuted matrices were used in each case, each subjected to TNT searches as above.

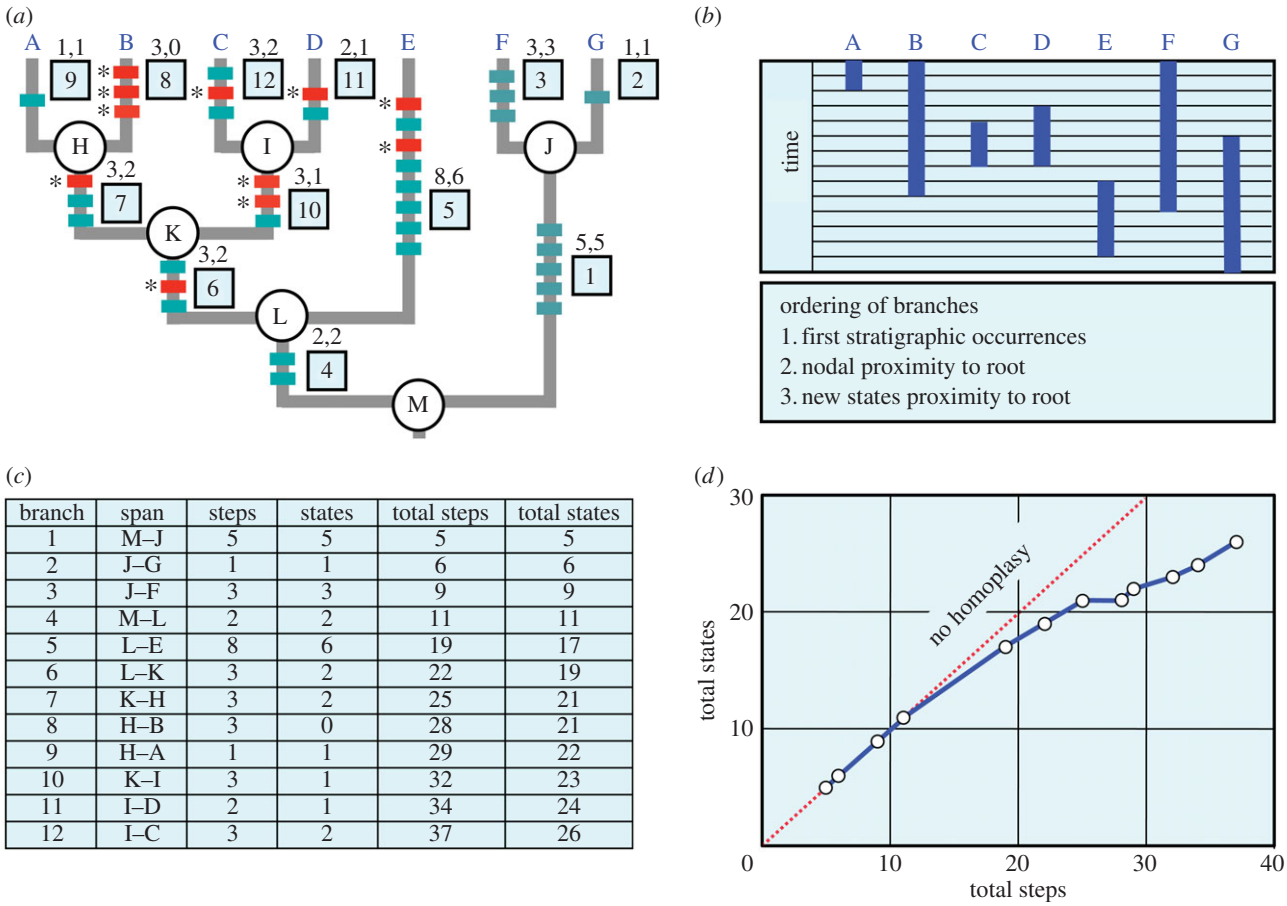

branch	span	steps	states	total steps	total states
1	M–J	5	5	5	5
2	J–G	1	1	6	6
3	J–F	3	3	9	9
4	M–L	2	2	11	11
5	L–E	8	6	19	17
6	L–K	3	2	22	19
7	K–H	3	2	25	21
8	H–B	3	0	28	21
9	H–A	1	1	29	22
10	K–I	3	1	32	23
11	I–D	2	1	34	24
12	I–C	3	2	37	26

Figure 1. Generating character saturation curves. (*a*) Step 1: ancestral states are reconstructed on a phylogeny in order to determine character transitions along each branch. Horizontal bars on branches indicate character state changes. Asterisks denote homoplastic changes (steps) that are not also new states. Branches are numbered within squares, and pairs of numbers above these indicate number of steps and number of novel states respectively. (*b*) Step 2: branches are ordered by stratigraphic occurrence, proximity to the root and number of new states. (*c*) Step 3: the number of steps and new states along each branch in the resulting sequence (denoted by the values in boxes) are calculated, along with running totals. (*d*) Step 4: the cumulative total of new states is plotted against the cumulative total of steps to generate a saturation curve. The dotted line indicates the trajectory (gradient of 1.0) for the hypothetical situation where there is no homoplasy, and all steps are novel states. (Online version in colour.)

Character exhaustion analyses were performed using the method and scripts of Wagner [58] (figure 1). Character states for ancestral nodes were reconstructed using Fitch parsimony [71], and all nodes were numbered. A traversal of the tree from the root to the terminal branches was used to tally a cumulative total of character change steps and novel states. Working from the basal node, branches were added in order of their stratigraphic age (as given by the age of the oldest fossil representative of the clade that the branch leads to), then by their nodal proximity to the root, and finally according to the smallest numbers of novel states evolving along them. As fossil data are unavailable for unsampled internal nodes, many of the internal branches could not be ordered by stratigraphic age and so were ranked according to the last two criteria. This does leave ties. For example, consider six taxa that appear in the same stratigraphic interval with hypothesized relationships ((A,(B,C)),(D,(E,F)). The basal node necessarily precedes the (A,(B,C)) and (D,(E,F)) nodes, and those two nodes necessarily precede the (B,C) and (E,F) nodes, respectively. However, neither the (A,(B,C)) nor (D,(E,F)) sister nodes necessarily precede each other [72], and the 'cousin' nodes (B,C) and (E,F) cannot be ordered relative to each other either. Therefore, such sister-taxon and 'Xth cousin' ties were resolved randomly, but with second cousin nodes preceding third cousin nodes. This ordering strategy is the most exact possible without recourse to stratigraphic data of higher resolution to subdivide branches. Such data are unavailable for the vast majority of our sampled clades. In addition, it is not uncommon for multiple fossil taxa to have their first occurrences at the same locality, resulting in ties, regardless of the temporal resolution available. Another approach would be to use arbitrary evolutionary models to calibrate branch lengths [73–75], and to assign character changes between known occurrences [76]. However, such models will bias results towards favouring character exhaustion. Longer branches with more novel character states will be pulled closer to the root, causing novel states to appear earlier in evolutionary time. This will be more pronounced if rate-variation among characters is permitted, because characters with a greater number of novel states will evolve at a faster rate, thereby concentrating the novel state changes on branches with deeper divergence times. In addition, it has been shown that different branch scaling methods can markedly influence the evolutionary inferences derived from trees [77]. Our approach is therefore a conservative one, insofar as it is more likely to defer the appearance of novel character states until later in our character exhaustion curves (inferred exhaustion will be less marked) and is not contingent upon arbitrary models of character evolution.

For each branch in the ranked sequence, the total number of character state changes (steps) and the total number of novel character states (states) was calculated and added to the cumulative total. Plotting the cumulative number of states against the cumulative number of steps yielded a states/steps curve for each of the 93 clades.

All subsequent analyses were implemented in R (v. 3.0.1) [61]. The shape of each states/steps curve was quantified in two ways (figure 2). First, we recorded the fraction of total observed steps at which an arbitrary threshold (50%) of the maximum number of

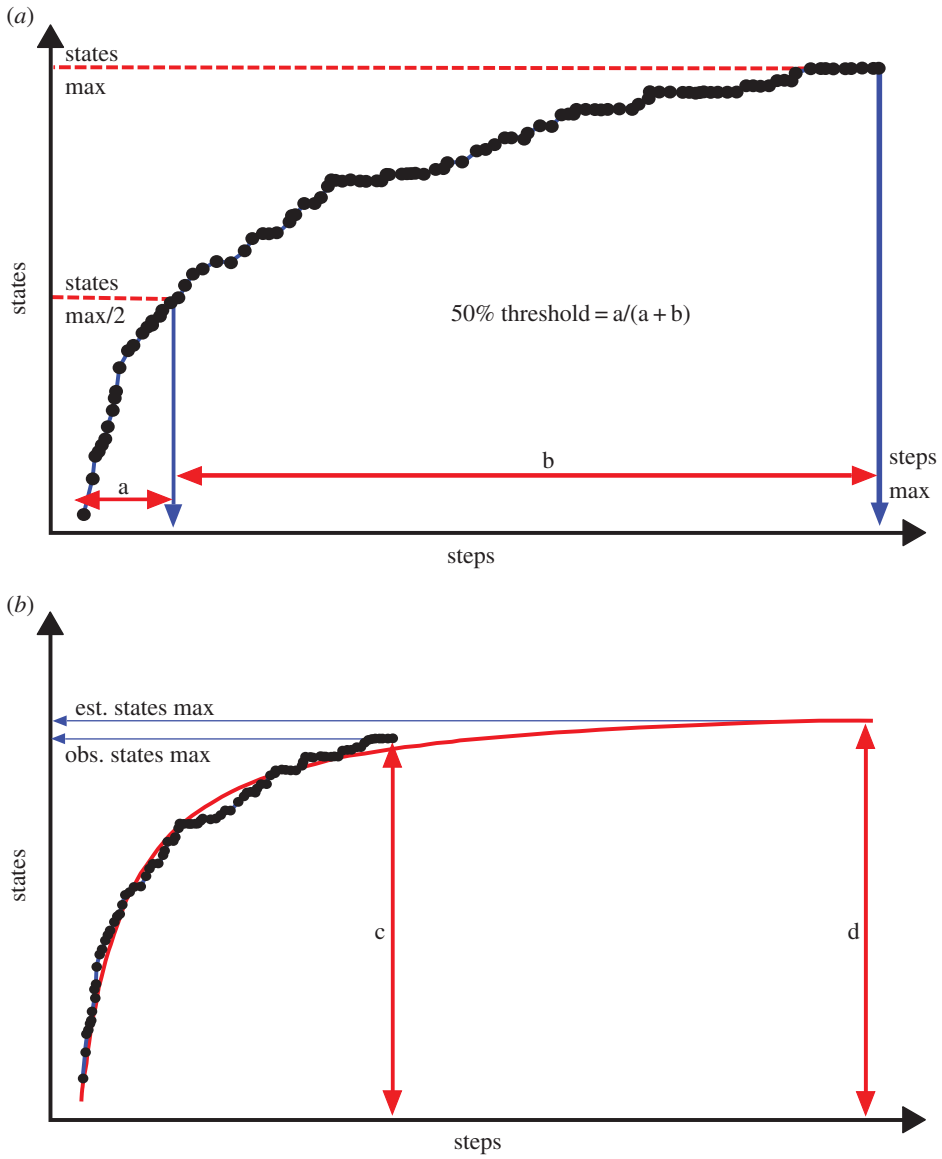

Figure 2. Quantifying character saturation from state/steps curves. (*a*) The 50% threshold is defined as the number of steps taken to reach 50% of the total number of character states (a) divided by the total number of observed steps (a + b). (*b*) The fraction of maximum states is defined as the total number of observed character states (c) divided by the estimated maximum number of possible character states (d) from the asymptote of the Michaelis–Menten curve. (Online version in colour.)

observed states was reached. Second, we calculated the CG for each states/steps curve (in an analogous manner to the CG for disparity profiles) and scaled this relative to the number of steps in the clade. The most convex curves with the highest initial gradients (i.e. those more quickly approaching an asymptote) yielded the lowest values for both indices. We also estimated the overall degree of saturation at clade extinction by fitting Michaelis–Menten nonlinear regression curves [78–80] to the data based on the assumption that the number of character states would eventually reach an asymptote (i.e. that the character space was finite). We then expressed the maximum number of observed states as a fraction of the inferred maximum. Low values in this context indicated clades that were further from saturation at their extinction.

Finally, each dataset was fitted to Wagner's idealized models of character evolution [58]. Log-likelihood values were used to assess whether a null model of a step-independent (linear) model of character evolution could be rejected in favour of step-dependent models indicating exhaustion.

3. Results

All summary statistics are given in table 1. Of our 93 sampled clades, only two realized the maximum intertaxon Euclidean distance for the entire morphospace within a single time bin. Most appeared relatively free to evolve within the morphospatial bounds, with a mean maximum observed distance (as a fraction of the maximum possible) of 0.712. HERs had a mean of 0.470 with a fairly typical distribution [55,56]. States/steps curves exhibited a range of shapes although most were asymptotic and reached a slope less than 1 (figure 3), indicating that some degree of character state saturation occurred in most groups. Of the 68 clades tested for fit with Wagner's models, the null model of a linear increase in new character states was rejected in 60 cases. Although nearly all clades showed a decrease in the rate at which new states appeared after about 30% of the maximum number of steps, 12 maintained a much reduced but constant rate of addition of states over the remainder of their evolutionary history (e.g. cinctans; figure 3*c*). Some groups, such as Aplodontoidea (mammalia; figure 3*f*), had stepped patterns, indicating that the origin of novel states was concentrated in a relatively small number of branches equidistant from the root. This is similar to the pattern recently documented within post-Palaeozoic echinoids [177]. The mean fraction of steps at which 50% of states were realized was 0.307, with

Table 1. Summary metrics for the 93 clades in the dataset. Ext: N = does not terminate coincident with a mass extinction boundary; Y = does terminate coincident with a mass extinction boundary. HER: homoplasy excess ratio. T50%: 50% threshold for character states. SCG: Saturation CG. Fchar: fraction of total character states relative to the estimated maximum from Michaelis–Menten asymptotes. CG: Disparity profile centre of gravity. CDev: Summed centroid deviance. Euc: Maximum Euclidean distance between taxa in any given time bin as a fraction of the maximum across all time bins. W: Top, significantly top heavy; Bot, significantly bottom heavy; N, CG neither top nor bottom heavy. ESat: Y, disparity in the first two stages not significantly different from maximum; N, disparity in the first two stages significantly different from maximum. LSat: Y, disparity in the last two stages not significantly different from maximum; N, disparity in the last two stages significantly different from maximum. Clades that realize the maximum inter-taxon Euclidean distance are highlighted in italic.

author	clade	extinct	HER	T50%	SCG	Fchar	CG	Cdev	Euc	W	ESat	LSat
Anderson *et al.* [81]	Acanthodii	N	0.796	0.292	0.635	0.509	0.446	1.492	0.837	Top	N	Y
Sigurdsen & Bolt [82]	Amphibamidae	N	0.240	0.607	0.658	0.274	0.316	1.755	0.601	N	Y	Y
Hill *et al.* [83]	Ankylosauria	Y	0.377	0.209	0.585	0.712	0.687	6.010	0.750	N	Y	Y
Fröbisch [84]	Anomodontia	N	0.602	0.254	0.602	0.672	0.511	2.618	0.765	Top	N	Y
Hopkins [85]	Aplodontoidea	N	0.626	0.136	0.593	0.820	0.185	3.307	0.764	N	N	Y
Dupret *et al.* [86]	Arthrodira	N	0.565	0.147	0.571	0.774	0.566	3.425	0.715	Bot	N	N
Fortey & Chatteron [87]	Asaphina	Y	0.502	0.438	0.693	0.255	0.611	1.753	0.803	N	N	Y
Lieberman & Kloc [88]	Asteropyginae	Y	0.194	0.233	0.605	0.718	0.641	2.434	0.713	Top	N	Y
Alvarez *et al.* [89]	Athyridida	N	0.236	0.302	0.627	0.723	0.526	2.910	0.690	Top	N	Y
Milner *et al.* [90]	Baphetoidea	N	0.095	0.266	0.599	0.639	0.451	0.685	0.909	N	N	Y
Benedetto [91]	Billingsellidina	N	0.393	0.308	0.620	0.575	0.734	2.968	0.700	N	Y	N
Bodenbender & Fisher [92]	Blastoidea	N	0.311	0.153	0.588	0.834	0.609	4.058	0.662	Top	N	Y
Foote [93]	Blastozoans	Y	0.623	0.115	0.585	0.896	0.477	3.149	0.685	Top	N	Y
Wang *et al.* [94]	Borophaginae	N	0.710	0.447	0.645	0.344	0.502	1.690	0.698	Bot	Y	N
Gaffney *et al.* [95]	Bothremydidae	N	0.587	0.335	0.633	0.544	0.471	2.027	0.512	N	N	N
Schoch & Milner [96]	Branchiosauridae	N	0.532	0.301	0.601	0.593	0.269	1.752	0.792	N	Y	Y
Mihlbachler & Deméré [97]	Brontotheriidae	N	0.549	0.103	0.614	0.860	0.415	2.658	0.516	N	Y	N
Jimenez-Sanchez *et al.* [98]	Bryozoa (unnamed clade)	N	0.234	0.286	0.595	0.645	0.427	3.247	0.669	N	Y	N
Sampson *et al.* [99]	Chasmosaurinae	Y	0.665	0.283	0.612	0.604	0.458	0.644	0.533	Bot	N	Y
Smith & Zamora [100]	Cinctans	N	0.470	0.353	0.607	0.440	0.477	1.201	0.637	N	Y	Y
Carlson & Fitzgerald [101]	Cryptonelloidea	N	0.277	0.331	0.620	0.568	0.399	3.154	0.587	Bot	N	N
Novas *et al.* [102]	Deinonychosauria	Y	0.607	0.334	0.603	0.541	0.635	5.566	0.720	Top	N	N
Wenwei *et al.* [103]	Dimeropygidae	Y	0.539	0.371	0.610	0.551	0.528	0.722	0.697	N	Y	Y
Clement & Long [104]	Dipterimorpha	N	0.417	0.268	0.584	0.681	0.225	3.881	0.753	Bot	Y	N
Foote [105]	Disparida	N	0.276	0.146	0.575	0.803	0.490	2.820	0.506	Bot	Y	N
Cotton & Fortey [106]	Eodiscina	N	0.291	0.129	0.576	0.865	0.375	2.118	0.594	Bot	Y	N

(*Continued.*)

Table 1. (*Continued.*)

author	clade	extinct	HER	T50%	SCG	Fchar	CG	Cdev	Euc	W	ESat	LSat
Maletz *et al*. [107]	Eugraptoloida	N	0.861	0.260	0.631	0.567	0.563	2.093	0.646	N	N	Y
Bloch *et al*. [108]	Euprimateforms	N	0.416	0.358	0.594	0.613	0.348	2.897	0.623	Bot	Y	N
Tetlie & Cuggy [109]	Eurypterina	N	0.553	0.323	0.639	0.525	0.509	3.677	0.787	N	Y	Y
Foote [105]	Flexibilia	Y	0.339	0.213	0.612	0.755	0.506	2.855	0.493	N	N	Y
Zhu & Gai [110]	Galeaspida	N	0.659	0.279	0.582	0.601	0.549	4.357	0.729	N	Y	Y
Korn [111]	Goniatitaceae	N	0.737	0.500	0.628	0.270	0.569	3.519	0.866	N	N	N
Gebauer [112]	Gorgonopsia	Y	0.697	0.422	0.635	0.424	0.514	0.694	0.991	N	Y	Y
Prieto-Marquez [113]	Hadrosauroidea	Y	0.639	0.268	0.604	0.656	0.700	0.407	0.708	Top	N	N
Wang [114]	Hesperocyoninae	N	0.636	0.481	0.704	0.404	0.520	3.467	0.668	N	N	Y
Polly [115]	Hyaenodontidae	N	0.454	0.370	0.622	0.501	0.540	1.627	0.797	N	N	Y
Motani [116]	Ichthyopterygia	N	0.699	0.372	0.614	0.415	0.359	5.625	0.770	Bot	Y	N
Trinajstic & Dennis-Bryan [117]	Incisoscutoidea	N	0.448	0.261	0.602	0.703	0.498	1.438	0.689	N	Y	Y
Sundberg [118]	Kochaspid Trilobites	N	0.122	0.313	0.650	0.561	0.485	1.225	0.660	N	Y	N
Adrain *et al*. [119]	*Koneprusiinae*	*N*	*0.399*	*0.240*	*0.634*	*0.687*	*0.755*	*4.519*	*1.000*	*N*	*Y*	*Y*
Klembara *et al*. [120]	Labyrinthodontia	N	0.301	0.214	0.576	0.706	0.368	2.492	0.658	N	N	N
Anderson *et al*. [121]	Lepospondyli	N	0.341	0.196	0.611	0.816	0.484	10.245	0.620	N	N	N
Pollitt *et al*. [122]	Lichoidea	Y	0.334	0.195	0.592	0.749	0.555	6.289	0.752	Bot	Y	N
Yates & Warren [123]	Limnarchia	N	0.344	0.224	0.599	0.741	0.437	4.957	0.640	N	Y	N
Hoffmann [124]	*Lytoceratoidea*	*Y*	*0.835*	*0.500*	*0.655*	*0.428*	*0.468*	*2.287*	*1.000*	*Bot*	*Y*	*N*
Damiani [125]	Mastodonsauroidea	N	0.342	0.302	0.575	0.533	0.394	2.592	0.726	Bot	Y	N
Young & De Andrade [126]	Metriorhynchoidea	N	0.869	0.332	0.639	0.489	0.451	5.418	0.780	N	N	N
Polly *et al*. [127]	Miacoidea	N	0.352	0.397	0.648	0.398	0.638	2.452	0.606	N	Y	Y
Ruta & Coates [128]	Microsauria	N	0.608	0.304	0.609	0.580	0.571	6.851	0.482	Bot	Y	Y
Lee *et al*. [129]	Missisquoiidae	N	0.096	0.214	0.598	0.742	0.379	2.828	0.761	N	N	Y
Bell Jr. & Polcyn [130]	Mosasauridae	Y	0.480	0.252	0.605	0.714	0.509	1.369	0.712	N	N	N
Kielan-Jaworowska & Hurum [131]	Multituberculata	N	0.465	0.310	0.628	0.540	0.520	3.535	0.774	Bot	Y	N
Pol *et al*. [132]	Notosuchia	N	0.435	0.353	0.621	0.482	0.355	3.968	0.500	N	N	Y
Lieberman [133]	Olenellina	N	0.147	0.276	0.625	0.666	0.507	0.698	0.732	N	Y	N
Lieberman [134]	Olenelloidea	N	0.083	0.265	0.604	0.728	0.481	1.411	0.658	N	N	N

(*Continued.*)

Table 1. (*Continued.*)

author	clade	extinct	HER	T50%	SCG	Fchar	CG	Cdev	Euc	W	ESat	LSat
Bajpai *et al*. [135]	Omomyoidea	N	0.222	0.190	0.592	0.790	0.497	8.393	0.446	Top	N	N
McDonald *et al*. [136]	Ornithopoda	Y	0.691	0.176	0.598	0.764	0.620	1.076	0.992	Top	N	Y
Mitchell [137]	Orthograptidae	Y	1.000	0.529	0.645	0.067	0.628	1.338	0.626	N	Y	Y
Sansom [138]	Osteostraci	N	0.552	0.266	0.599	0.682	0.499	2.894	0.520	Top	N	N
Longrich *et al*. [139]	Pachycephalosauria	Y	0.480	0.442	0.625	0.469	0.631	1.791	0.655	Bot	N	N
Prokop & Ren [140]	Palaeodictyoptera	N	0.077	0.314	0.625	0.521	0.351	2.316	0.861	Bot	Y	N
Jin & Popov [141]	Parastrophinidae	N	0.414	0.321	0.612	0.652	0.118	4.577	0.565	N	Y	Y
Stocker [142]	Parasuchia	Y	0.374	0.329	0.618	0.489	0.496	0.369	0.761	N	Y	N
Lopez-Arbarello & Zavattieri [143]	Perleidiformes	Y	0.346	0.213	0.604	0.730	0.471	1.422	0.791	Top	Y	N
Smith & Pol [144]	Plateosauria	N	0.426	0.450	0.628	0.761	0.672	2.313	0.771	N	N	Y
Anderson *et al*. [81]	Placodermi	Y	0.638	0.271	0.584	0.528	0.560	2.515	0.650	N	N	N
Ketchum & Benson [145]	Plesiosauria	Y	0.375	0.264	0.606	0.709	0.509	3.684	0.762	N	Y	Y
Smith & Dyke [146]	Pliosauroidea	Y	0.616	0.274	0.596	0.693	0.506	3.001	0.743	N	Y	Y
Cisneros & Ruta [147]	Procolophonidae	Y	0.581	0.355	0.648	0.517	0.486	2.387	0.650	N	Y	Y
Huguet *et al*. [148]	Protomyrmeleontidae	Y	0.046	0.305	0.629	0.585	0.435	2.051	0.851	Bot	Y	N
Nel *et al*. [149]	Protanisoptera	N	0.478	0.313	0.576	0.563	0.451	1.732	0.949	N	Y	N
Egi *et al*. [150]	Proviverrinae	N	0.214	0.297	0.634	0.557	0.184	4.303	0.773	Top	Y	Y
Parker & Irmis [151]	Pseudopalatinae	Y	0.572	0.333	0.619	0.471	0.641	1.104	0.811	N	Y	Y
Pernègre & Elliott [152]	Pteraspidiformes	N	0.336	0.248	0.586	0.644	0.471	1.492	0.709	N	N	Y
Lü *et al*. [153]	Pterosauria	Y	0.545	0.315	0.616	0.515	0.529	2.626	0.679	N	Y	N
Poyato-Ariza & Wenz [154]	Pycnodontiformes	N	0.279	0.308	0.627	0.568	0.487	1.878	0.590	N	Y	Y
Brusatte *et al*. [155]	Rauisuchia	N	0.517	0.388	0.619	0.501	0.508	3.310	0.753	N	N	N
Bates *et al*. [156]	Retiolitidae	N	0.578	0.333	0.623	0.517	0.557	2.765	0.704	N	N	N
Cerdeno [157]	Rhinocerotidae	N	0.327	0.131	0.586	0.831	0.517	2.379	0.772	N	Y	N
Hone & Benton [158]	Rhyncosauria	Y	0.764	0.411	0.587	0.365	0.568	2.877	0.880	N	Y	Y
Allain & Aquesbi [159]	Sauropoda	Y	0.538	0.380	0.606	0.478	0.539	3.850	0.774	Bot	Y	Y
Maidment [160]	Stegosauria	N	0.652	0.625	0.673	0.102	0.338	1.422	0.602	Bot	N	N
Carlson & Fitzgerald [101]	Stringocephaloidea	N	0.352	0.279	0.617	0.436	0.473	2.562	0.739	Bot	N	N
Schoch [161]	Stereospondyli	N	0.474	0.409	0.641	0.659	0.354	4.755	0.650	Bot	N	N

(*Continued.*)

Table 1. (*Continued.*)

author	clade	extinct	HER	T50%	SCG	Fchar	CG	Cdev	Euc	W	ESat	LSat
Lamsdell *et al.* [162]	Stylonurina	N	0.541	0.259	0.612	0.673	0.470	5.966	0.629	N	N	Y
Klug [163]	Synechodontiformes	N	0.641	0.288	0.627	0.645	0.617	1.561	0.200	Top	N	N
Gaudin [164]	Tardigrada	N	0.466	0.201	0.589	0.691	0.641	6.917	0.669	N	N	Y
Wu *et al.* [165]	Thalattosauria	Y	0.560	0.414	0.622	0.376	0.533	0.967	0.951	Top	N	N
Wilson & Märss [166]	Thelodonti	N	0.387	0.249	0.611	0.607	0.587	3.898	0.729	Top	Y	N
Hu *et al.* [167]	Theropoda	Y	0.422	0.300	0.611	0.567	0.579	2.125	0.971	N	N	N
Chatterton *et al.* [168]	Toemquistidae	Y	0.141	0.308	0.593	0.593	0.462	0.793	0.653	Top	N	Y
Brusatte *et al.* [169]	Tyrannosauroidea	Y	0.778	0.372	0.645	0.405	0.633	3.267	0.950	Bot	N	N
Anderson & Seldon [170]	Xiphosura	N	0.896	0.575	0.590	0.076	0.266	4.934	0.803	Bot	N	N

values ranging between 0.103 (the most convex curve with fastest saturation) and 0.625 (the most nearly linear curve with the least saturation). Michaelis–Menten curve fits all inferred asymptotes in excess of the realized maximum at extinction; observed maxima varied between 0.067 and 0.896 of the inferred, with a mean of 0.583. These two indices of state saturation were strongly negatively and highly significantly correlated ($r_s = -0.873$, $p < 0.001$; those clades taking longest to reach 50% of the realized maximum tended to be those in which the realized maximum was the smallest fraction of the inferred, because the empirical curves were truncated by extinction at the steepest gradients). CG indices for the empirical curves showed a narrow range of values as expected (0.571–0.704), but correlated highly significantly with both the empirical 50% thresholds ($r_s = 0.631$, $p < 0.001$) and the realized fraction of inferred states ($r_s = -0.578$, $p < 0.001$).

There was a weak but significant negative correlation between overall homoplasy levels and the disparity CG ($r_s = 0.227$, $p < 0.029$): clades with a lower CG (earlier higher disparity) had greater homoplasy (lower HER) on average (figure 4). However, we found no significant relationships between disparity CG and any of our indices of saturation curve shape ($r_s = 0.008$, $p = 0.941$ for the 50% threshold; $r_s = 0.091$, $p = 0.388$ for the saturation curve CG; $r_s = -0.039$, $p = 0.708$ for the Michaelis–Menten estimate of the realized fraction of inferred states). Limiting the analysis to wholly extinct clades that did not terminate coincident with a mass extinction boundary resulted in weaker correlations for all indices of character saturation except the 50% threshold point (table 2). Finally, analysis of the CG of clades terminating at mass extinction boundaries yielded similar results for indices of character exhaustion but showed no correlation with HER values. Maximum Euclidean distance within a time bin correlated negatively with the Michaelis–Menten estimates of the realized fraction of inferred states ($r_s = -0.229$; $p = 0.027$), indicating that character saturation may be greater in clades that reach their morphospatial bounds. However, no correlation was found between character saturation metrics and the amount of centroid deviation (50% threshold: $r_s = -0.173$, $p = 0.097$; saturation CG: $r_s = -0.183$, $p = 0.079$ fraction of inferred states $r_s = 0.198$, $p = 0.057$) implying that clades that migrate through the morphospace are as likely to show saturation as those that statically occupy a defined region. The morphospace of clades that show early disparity and similar saturation values (figure 5) reveals that some clades continue to evolve new character states as they migrate through the morphospace (e.g. disparid crinoids), whereas others remain fixed and occupied space within existing bounds (e.g. lichoid trilobites). Whether a clade showed early or late high-disparity also had no effect on the degree of character exhaustion within that clade (table 3).

4. Discussion

The significant but weak correlation between disparity CG and overall levels of homoplasy demonstrates that clades with higher disparity earlier in their histories are more likely to show higher levels of character state reversal and convergence. While this implies the operation of some constraint or restriction (*sensu* Wagner [6]), the small size of the effect ($R^2 = 0.030$ if modelled linearly) suggests that some other factor or factors are much more important. The absence of

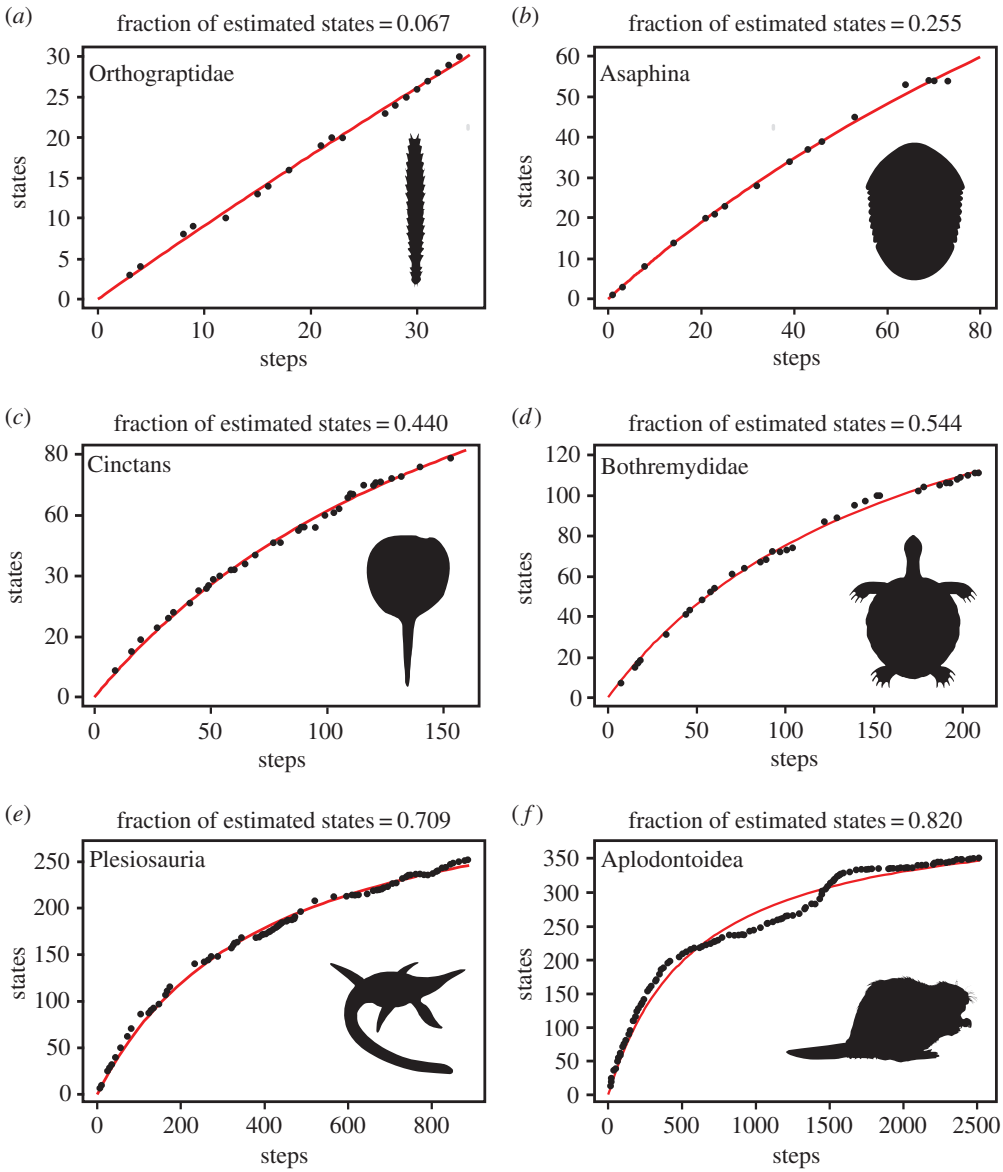

Figure 3. Example Michaelis–Menten functions fitted to state/steps data for different extinct animal clades. See text for explanation of how the fraction of estimated maximum number of states was calculated. Points indicate cumulative totals as each branch is added. (*a*) Orthograptidae [171]. (*b*) Asaphina [172]. (*c*) Cinctans [173]. (*d*) Bothremydidae [174]. (*e*) Plesiosauria [175]. (*f*) Aplodontoidea [176]. (Online version in colour.)

significant correlation between disparity CG and any of our proxies for states/steps curve shape indicates that disparity is not shaped in any straightforward way by progressive exhaustion of the character space. Patterns of disparity through time cannot therefore be deduced straightforwardly from patterns of homoplasy increase throughout the lifetime of clades, and are only weakly influenced by overall homoplasy levels. Many clades continue to evolve new character states with no associated increase in their disparity, whereas others achieve their highest levels of disparity through homoplastic character change. Several clades (including crustaceans and priapulid worms [180,181]) occupy a similarly sized morphospace envelope throughout much of their evolution (similar disparity), but nevertheless migrate through the overall morphospace. Other clades (e.g. angiosperms, Jurassic ammonoids [182]) quickly colonize many of the morphospatial extremes (reaching maximum disparity) but subdivide the envelope progressively through time and continue to evolve new states. The major axes of our empirical morphospaces are likely to be defined by the principal patterns of covariation between character states, and it is these patterns that largely determine Euclidean eccentricity from the global centroids. Similarly, the most eccentric (extreme) morphologies may embody sets of character states that have individually evolved earlier in the history of the clade, but never before in combination. Upon its first evolution, a new state need not necessarily move a lineage to a particularly eccentric position in the morphospace, neither will it necessarily result in the expansion of the morphospace occupied by contemporaneous taxa, particularly where the space is contracting on other fronts.

In most of our sampled clades, new character states continued to evolve long after maximum disparity had been reached. Major groups often share a conserved morphological template or bodyplan (Bauplan), usually defined by character changes at the clade's base. This implies that some characters are relatively invariant or become 'fixed', whereas other characters continue to evolve new states. Neither conventional morphospace analyses nor our states/steps curves distinguished between characters on the basis of their evolutionary or developmental depth. State changes might therefore range from fundamental shifts in body symmetry and organization (more typical of those delimiting phyla), down to subtle changes in bristle patterns at the other (perhaps more typical of species), yet all contribute equally. Furthermore, as cladistic matrices are

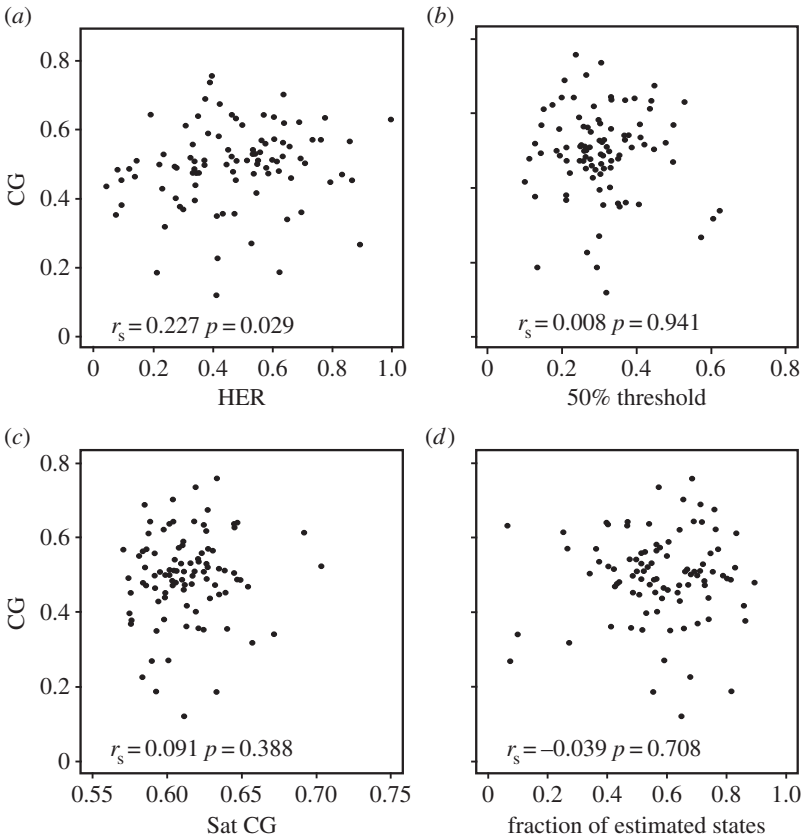

Figure 4. Disparity profile centre of gravity (CG) plotted against homoplasy excess ratio (HER) and estimates of character saturation. (*a*) Disparity CG versus HER. (*b*) Disparity CG versus 50% threshold. (*c*) Disparity CG versus saturation curve CG. (*d*) Disparity CG versus fraction of the Michaelis-Menten estimate of the maximum number of character states realized at extinction. r_s and *p*-values are from Spearman's rank correlation coefficient tests.

Table 2. *p*-values from Spearman rank tests for homoplasy excess ratio (HER) and three proxies of character exhaustion (fraction of the total number of steps at which 50% of states are realized, CG of the saturation curve, and the fraction of the estimated number of states (inferred from Michaelis–Menten curve) that are observed) correlated with disparity profile CG. Values are calculated for the entire dataset of 93 clades, the subset of 55 clades not becoming extinct coincident with a mass extinction boundary and that have no extant survivors, and the subset of 31 clades that terminate at a mass extinction boundary.

	HER	50% threshold	saturation curve CG	observed maximum states/ estimated maximum states
disparity CG (entire dataset, $n = 93$)	$r_s = 0.227$ $p = 0.029$	$r_s = 0.008$ $p = 0.941$	$r_s = 0.091$ $p = 0.388$	$r_s = 0.039$ $p = 0.708$
disparity CG (clade extinction not coincident with mass extinction, $n = 55$)	$r_s = 0.285$ $p = 0.035$	$r_s = -0.107$ $p = 0.436$	$r_s = 0.010$ $p = 0.940$	$r_s = 0.037$ $p = 0.786$
disparity CG (clade extinction coincident with mass extinction $n = 31$)	$r_s = 0.085$ $p = 0.649$	$r_s = 0.145$ $p = 0.438$	$r_s = 0.099$ $p = 0.597$	$r_s = 0.094$ $p = 0.614$

created with the express purpose of inferring relationships, the characters within such matrices will primarily be synapomorphies of subclades. Deep synapomorphies (which may be shared by all members of the focal clade) will usually be absent, because they contain no useful phylogenetic information. For example, characters such as the presence and absence of limbs or a notochord will not be included in a dataset of vertebrates that all share these derived features. As a result, cladistic datasets are likely to under-represent characters subjected to strong intrinsic constraints, which have already become 'fixed' within the clade of interest. For this and other reasons, conventional discrete character morphospaces—and the estimates of disparity derived from them—may not be best suited for recognizing the changes of deepest developmental and evolutionary significance. Morphospaces that take account of the developmental depth of characters have long been called for [3], and some moves have been made towards realizing these for particular clades [48,183–186].

Several authors have distinguished between intrinsic and extrinsic limits to disparity [7], with intrinsic factors being those that operate within the individuals and lineages that constitute a clade (broadly equating to geometric and developmental constraints) and extrinsic or ecological factors being those imposed from the outside (biological and physical restrictions) [6,26]. The precise limits on the evolution of disparity are probably unique to each clade, and comprise some combination of factors. Determining the relative importance of these is not straightforward, and direct tests are

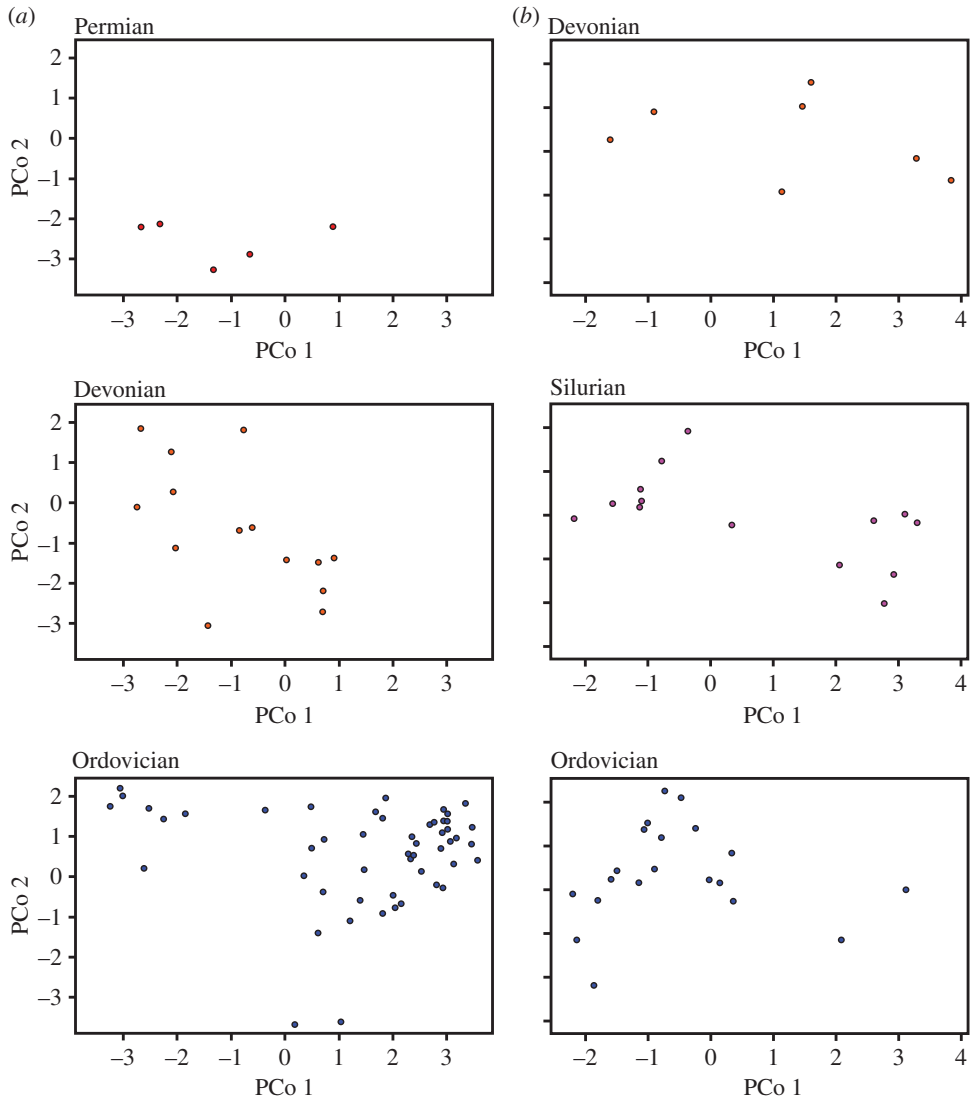

Figure 5. Differing patterns of morphospace occupation along the first two principal coordinate axes in clades showing early high-disparity. CG: disparity profile centre of gravity. Fchar: fraction of total realized character states relative to the maximum estimated from Michaelis–Menten asymptotes. Euc: maximum Euclidean distance between taxa in any given time bin as a fraction of the maximum across all time bins. (*a*) Disparid crinoids from Foote [178] (CG = 0.490, FChar = 0.803, Euc = 0.506) showing migration through the morphospace. PCo 1 = 23.6% total variance, PCo 2 = 12.0% total variance. (*b*) Lichoid trilobites from Pollitt *et al.* [179] (CG = 0.555, FChar = 0.749, Euc = 0.752) showing more static occupation of the morphospace. PCo 1 = 26.2% total variance, PCo 2 = 13.4% total variance. (Online version in colour.)

Table 3. Summary statistics from Mann–Whitney *U* tests of differences between median homoplasy excess ratio (HER) and three character saturation metrics (fraction of the total number of steps at which 50% of states are realized, CG of the saturation curve, and the fraction of the estimated number of states (inferred from Michaelis–Menten curve) that are observed) when bi-partitioned by disparity profile shape. Bottom heavy versus top heavy: clades grouped based on a CG value significantly higher or lower than mean randomized values (with other clades omitted). Early maximum disparity: clades partitioned according to whether or not they show disparity in the first two stages that is significantly different from the maximum. Late maximum disparity: clades partitioned according to whether or not they show disparity in the last two stages that is significantly different from the maximum.

	HER	50% threshold	saturation curve CG	observed maximum states/ estimated maximum states
significantly bottom heavy versus	$W = 216$	$W = 288$	$W = 219.5$	$W = 110$
significantly top heavy	$p = 0.588$	$p = 0.012$	$p = 0.520$	$p = 0.019$
early maximum disparity	$W = 1277.5$	$W = 989$	$W = 1077$	$W = 1189.5$
	$p = 0.131$	$p = 0.482$	$p = 0.979$	$p = 0.407$
late maximum disparity	$W = 997.5$	$W = 1095$	$W = 1005.5$	$W = 1051$
	$p = 0.535$	$p = 0.899$	$p = 0.580$	$p = 0.838$

impossible with the present data. There are some strongly suggestive patterns, however.

4.1. Intrinsic developmental constraints

As ontogeny becomes more complex, and genetic and other mechanisms become progressively more interdependent, increasing pleiotropy and functional linkage may result in developmental programmes that are more difficult to modify and subsequently evolve [187,188]. While some aspects of bodyplan organization may be strongly adaptive and maintained by stabilizing selection, other aspects may be largely contingent but locked down by the difficulty of effecting change in developmental programmes. The seven cervical vertebrae of mammals furnish the best-known example. Nearly all mammals—including the long-necked giraffes, gerenuks and alpacas—have just seven neck vertebrae. Other vertebrate groups retain the ability to modify this number, and invariably evolve longer necks with greater numbers of vertebrae; up to 25 in birds, 19 in sauropods [189] and 75 in the extinct plesiosaurs [190]. Two extant groups of mammals depart from the mammalian ground plan of seven; sloths have six (*Choloepus*) or eight or nine (*Bradypus*), whereas manatees (*Trichechus*) have six. All achieve this by homeotic frameshifts of the thoracic expression pattern (the development of ribs, etc.) relative to the underlying somites [191]. Such shifts in other mammals may be linked to highly deleterious, pleiotropic side effects, not least problems with the innervation, musculature and blood supply of the forelimbs and elevated rates of juvenile cancer [192]. Sloths and manatees appear to avoid these effects by low rates of metabolism and overall activity [178,192,193]. The pentadactyl limb of tetrapods is another example of a design that was apparently much more labile early in its evolution. Early labrynthodont tetrapods had higher numbers of digits: eight in the forelimbs of *Acanthostega*, seven in the hindlimbs of *Ichthyostega*, six in *Tulerpeton*. Modern lissamphibians—despite their ground plan of five digits—often develop greater numbers with no ill effects: ostensibly because limb patterning in aquatic larvae occurs prior to the phylotypic stage of development, during which time inductive interactions and interdependencies are concentrated. Many amniote groups, by contrast, have reduced digit numbers as adults (e.g. horses, non-avian dinosaurs, birds [179]), but few lineages have attained higher numbers, often evolving a variety of digit-like structures rather than extra digits *per se* [194,195]. Ichthyosaurs furnish the best-known exception: opthalmosaurians added digits anterior to digit one and posterior to digit five [196], whereas non-opthalmosaurians may have achieved polydactyly by interdigital or postaxial phalangeal bifurcation [197]. In most amniote groups, however, polydactyly is associated with a range of deleterious pleiotroipic effects [198–200], because limb development coincides with the phylotypic stage. Variation in this particular set of characters appears to be effectively locked down, therefore.

4.2. Extrinsic physical and biological (ecological) restrictions

In general, levels of clade disparity are often much less depleted by mass extinction events than levels of diversity. This is because numerous lineages can be lost from a morphospace while still maintaining a broad distribution of survivors [201]. Indeed, even where extinction selectively removes large subclades, disparity levels may remain high provided that the surviving clades occupy peripheral regions of the morphospace [202]. Where increases in levels of disparity coincide with marked and episodic changes in the physical or biological environment, it may be reasonable to infer that extrinsic, ecological constraints have been removed. Such shifts may occur in the immediate wake of mass extinctions, although in such cases, it may be difficult to distinguish the removal of biological constraints—for example, the extinction of competing or incumbent clades—from the physical environmental shifts that precipitate these biological changes. However, several of the largest and most conspicuous adaptive radiations have classically been understood in ecological terms. Crown group mammals evolved numerous new body forms (broadly equating to modern orders, and with many striking parallels between Eutheria and Metatheria in different settings) after the K/Pg mass extinction. This occurred not only in the aftermath of the extinction of the non-avian dinosaurs, but also coincident with the final demise of eutriconodont, spalacotheroid and multituberculate mammals [203]. Similarly, articulate brachiopods rapidly increased their disparity in the wake of the end Permian mass extinction; a pattern consistent with rebound after the removal of highly structured guilds and the freeing up of ecospace [204]. Comparable post-extinction rebounds have been observed for crinoid and blastozoan echinoderms [27], as well as ammonoids [205] through multiple events. Similarly, rapid increases in disparity may occur when a clade is first able to colonize a fundamentally new region of ecospace. Even bodyplans that are assembled piecemeal over many tens of millions of years may reach a critical threshold, thereby suddenly circumventing previous restrictions [41].

5. Conclusion

In addition to studying the phylogeny and diversity of clades throughout their evolution [21,25,30], it is increasingly common to examine the manner in which groups explore theoretical or empirical morphospaces through time [43,184], as well as their resulting temporal patterns of morphological disparity change. Disparity and diversity are fundamentally decoupled [29], and a variety of trajectories have been observed empirically. The most common pattern, however, is for disparity to peak relatively early in the history of a clade, and certainly before its peak in diversity [7]. Putative limits on disparity may either be intrinsic (e.g. developmental [48,193]) or extrinsic (e.g. ecological [27,204,205]), but both imply constraints on available morphospace that might be reflected in the rate of evolution of novel morphology throughout the lifetime of a clade. The majority of clades studied do indeed show a significant decrease in the rate of appearance of novel character states over time. However, despite a weak correlation between overall levels of homoplasy (as measured by the HER) and the CG of clade disparity profiles (greater homoplasy implies earlier high-disparity) we found no more detailed relationships between the shapes of character saturation curves and disparity profiles. Many clades continue to evolve new character states while disparity levels remain constant, which can variously be achieved by wholesale migration through the morphospace or by subdividing it. Similarly, disparity may be increased or maximized by predominantly homoplastic state changes. The anecdotally large number of clades showing the expansion of hitherto restricted

morphospaces in the aftermath of mass extinctions (or upon transitioning into fundamentally new habitats) suggests that many of the limitations may be ecological. However, given the variation shown in both character saturation and morphospace occupation, limits on disparity almost certainly result from a complex interplay of clade-specific intrinsic and extrinsic factors, suggesting that a simple universal explanation for early high-disparity is unlikely.

Authors' contributions. J.W.O. co-wrote the paper, collected data, implemented analyses of homoplasy and character exhaustion and drafted figures. M.H. analysed disparity trajectories, collected data, wrote scripts and drafted figures. P.J.W. scripted the states/steps analyses and contributed to writing. S.G. analysed disparity trajectories. M.A.W. conceived the study, co-wrote the paper and drafted figures.

Competing interests. We have no competing interests.

Funding. This research was supported by grants from the John Templeton Foundation (43915), and from The Leverhulme Trust (F/00351/Z) awarded to M.A.W.

Acknowledgements. The authors thank Melanie Hopkins and an anonymous reviewer for constructive comments on an earlier draft of this paper. The authors were are also grateful to Alex Jeffries for instructive discussion and help in implementing Michaelis–Menten curves.

References

1. Ward PD, Signor PW. 1985 Evolutionary patterns of Jurassic and Cretaceous ammonites: an analysis of clade shape. In *Phanerozoic diversity patterns: profiles in macroevolution* (ed. JW Valentine), pp. 399–418. Princeton, NJ: Princeton University Press.
2. Gould SJ. 1989 *Wonderful life*. New York, NY: WW Norton.
3. Gould SJ. 1991 The disparity of the Burgess Shale arthropod fauna and the limits of cladistic analysis: why we must strive to quantify morphospace. *Paleobiology* **17**, 411–423. (doi:10.2307/2400754)
4. Valentine JW. 1990 The macroevolution of clade shape. In *Causes of evolution: a paleontological perspective* (eds RM Ross, WD Allmon), pp. 128–150. Chicago, IL: University of Chicago Press.
5. McShea DW. 1994 Mechanisms of large-scale evolutionary trends. *Evolution* (*NY*) **48**, 1747–1763. (doi:10.2307/2410505)
6. Wagner PJ. 2010 Paleontological perspectives on morphological evolution. In *Evolution since Darwin: the first 150 years* (eds MA Bell, DJ Futuyma, WF Eanes, JS Levinton), pp. 451–578. Sunderland, MA: Sinauer.
7. Hughes M, Gerber S, Wills MA. 2013 Clades reach highest morphological disparity early in their evolution. *Proc. Natl Acad. Sci. USA* **110**, 13 875–13 879. (doi:10.1073/pnas.1302642110)
8. Gould SJ, Calloway CB. 1980 Clams and brachiopods-ships that pass in the night. *Paleontology* **6**, 383–396.
9. Briggs JC. 1998 Biotic replacements: extinction or clade interaction?. *Bioscience* **48**, 389–395. (doi:10.2307/1313378)
10. Sepkoski JJ, McKinney FK, Lidgard S. 2000 Competitive displacement among post-Paleozoic cyclostome and cheilostome bryozoans. *J. Inf.* **26**, 7–18. (doi:10.1073/1666/0094-8373(2000)026<0007:cdappc>2.0.co;2)
11. Jablonski D. 2008 Biotic interactions and macroevolution: extensions and mismatches across scales and levels. *Evolution* (*NY*). **62**, 715–739. (doi:10.1111/j.1558-5646.2008.00317.x)
12. McGowan AJ, Dyke GJ. 2007 A morphospace-based test for competitive exclusion among flying vertebrates: did birds, bats and pterosaurs get in each other's space? *J. Evol. Biol.* **20**, 1230–1236. (doi:10.1111/j.1420-9101.2006.01285.x)
13. Pedersen RØ, Sandel B, Svenning J-C. 2014 Macroecological evidence for competitive regional-scale interactions between the two major clades of mammal carnivores (Feliformia and Caniformia). *PLoS ONE* **9**, e100553 (doi:10.1371/journal.pone.0100553)
14. Jablonski D. 2005 Mass extinctions and macroevolution. *Paleobiology* **31**, 192–210. (doi:10.1666/0094-8373(2005)031[0192:MEAM]2.0.CO;2)
15. Benton MJ. 1995 Diversification and extinction in the history of life. *Science* (*80-.*). **268**, 52–58. (doi:10.1126/science.7701342)
16. Benton MJ. 2001 Biodiversity on land and in the sea. *Geol. J.* **230**, 211–230. (doi:10.1002/gj.877)
17. Smith AB. 2007 Marine diversity through the Phanerozoic: problems and prospects. *J. Geol. Soc. Lond.* **164**, 731–745. (doi:10.1144/0016/76492006-184)
18. McGowan A, Smith AB. 2008 Are global Phanerozoic marine diversity curves truly global? A study of the relationship between regional rock records and global Phanerozoic marine diversity. *Paleobiology* **34**, 80–103. (doi:10.1666/07019.1)
19. Valentine JW, Jablonski D. 2010 Origins of marine patterns of biodiversity: some correlates and applications. *Palaeontology* **53**, 1203–1210. (doi:10.1111/j.1475-4983.2010.01005.x)
20. Ruta M, Cisneros JC, Liebrecht T, Tsuji LA, Müller J. 2011 Amniotes through major biological crises: faunal turnover among Parareptiles and the end-Permian mass extinction. *Palaeontology* **54**, 1117–1137. (doi:10.1111/j.1475-4983.2011.01051.x)
21. Benton MJ. 2009 The Red Queen and the Court Jester: species diversity and the role of biotic and abiotic factors through time. *Science* (*80-.*). **323**, 728–732. (doi:10.1126/science.1157719)
22. Nee S. 2006 Birth-death models in macroevolution. *Annu. Rev. Ecol. Evol. Syst.* **37**, 1–17. (doi:10.1146/annurev.ecolsys.37.091305.110035)
23. Foote M. 1991 Morphological patterns of diversification—examples from trilobites. *Palaeontology* **34**, 461–485.
24. Foote M. 1993 Discordance and concordance between morphological and taxonomic diversity. *Paleobiology* **19**, 185–204. (doi:10.2307/2400876)
25. Gould S, Gilinsky N, German R. 1987 Asymmetry of lineages and the direction of evolutionary time. *Science* (*80-.*), **236**, 1437–1441.
26. Erwin DH. 2007 Disparity: morphological pattern and developmental context. *Palaeontology* **50**, 57–73. (doi:10.1111/j.1475-4983.2006.00614.x)
27. Ciampaglio CN, Kemp M, McShea DW. 2001 Detecting changes in morphospace occupation patterns in the fossil record: characterization and analysis of measures of disparity. *Paleobiology* **27**, 695–715. (doi:10.1666/0094-8373(2001)027<0695:DCIMOP>2.0.CO;2)
28. Wills MA. 2001 Disparity vs. diversity. In *Palaeobiology II* (eds DEG Briggs, PR Crowther), pp. 495–500. Oxford, UK: Blackwell Science.
29. Foote M. 1992 Paleozoic record of morphological diversity in blastozoan echinoderms. *Proc. Natl Acad. Sci. USA* **89**, 7325–7329. (doi:10.1073/pnas.89.16.7325)
30. Foote M. 1997 The evolution of morphological diversity. *Annu. Rev. Ecol. Syst.* **28**, 129–152. (doi:10.1146/annurev.ecolsys.28.1.129)
31. Roy K, Foote M. 1997 Morphological approaches to measuring biodiversity. *Trends Ecol. Evol.* **1**, 277–281. (doi:10.1016/S0169-5347(97)81026-9)
32. Wills MA. 1998 Crustacean disparity through the Phanerozoic: comparing morphological and stratigraphic data. *Biol. J. Linn. Soc.* **65**, 455–500. (doi:10.1111/j.1095-8312.1998.tb01149.x)
33. Rabosky DL, Slater GJ, Alfaro ME. 2012 Clade age and species richness are decoupled across the eukaryotic tree of life. *PLoS Biol.* **10**, e1001381. (doi:10.1371/journal.pbio.1001381)
34. Foote M. 1991 Morphological and taxonomic diversity in clade's history: the blastoid record and stochastic simulations. *Contrib. From Museum Paleontol.* **28**, 101–140.
35. Foote M. 1996 Models of morphological diversification. In *Evol. Paleobiol.*, pp. 62–89. Chicago, IL: University Chicago Press.
36. Wills MA, Briggs DEG, Fortey RA. 1994 Disparity as an evolutionary index: a comparison of Cambrian and Recent arthropods. *Paleobiology* **20**, 93–130. (doi:10.2307/2401014)
37. Foote M. 1993 Contributions of individual taxa to overall morphological disparity. *Paleobiology* **19**, 403–419.
38. Foote M. 1996 Ecological controls on the evolutionary recovery of post-Paleozoic crinoids.

Science (*80-*.). **274**, 1492–1495. (doi:10.1126/science.274.5292.1492)

39. Wagner PJ. 1995 Testing evolutionary constraint hypotheses with early Paleozoic gastropods. *Paleobiology* **21**, 248–272.
40. Gerber S. 2013 On the relationship between the macroevolutionary trajectories of morphological integration and morphological disparity. *PLoS ONE* **8**, e63913. (doi:10.1371/journal.pone.0063913)
41. Brusatte SL, Lloyd GT, Wang SC, Norell MA. 2014 Gradual assembly of avian body plan culminated in rapid rates of evolution across the dinosaur-bird transition. *Curr. Biol*. **24**, 2386–2392. (doi:10.1016/j.cub.2014.08.034)
42. Schindel DE. 1990 Unoccupied morphospace and the coiled geometry of gastropods: architectural constraint or geometric covariation? In *Causes of evolution: a paleontological perspective* (eds RM Ross, WD Allmon), pp. 270–304. Chicago, IL: University of Chicago Press.
43. McGhee GR. 2006 *The geometry of evolution: adaptive landscapes and theoretical morphospaces*. Chicago, UK: Cambridge University Press.
44. Raup DM, Michelson A. 1965 Theoretical morphology of the coiled shell. *Science* (*80-*.). **147**, 1–2.
45. Wagner PJ, Erwin DH. 2006 Patterns of convergence in general shell form among Paleozoic gastropods. *Paleobiology* **32**, 316–337. (doi:10.1666/04092.1)
46. Serb JM, Alejandrino A, Otárola-Castillo E, Adams DC. 2011 Morphological convergence of shell shape in distantly related scallop species (Mollusca: Pectinidae). *Zool. J. Linn. Soc*. **163**, 571–584. (doi:10.1111/j.1096-3642.2011.00707.x)
47. Smith UE, Hendricks JR. 2013 Geometric morphometric character suites as phylogenetic data: extracting phylogenetic signal from gastropod shells. *Syst. Biol*. **62**, 366–385. (doi:10.1093/sysbio/syt002)
48. Gerber S. 2014 Not all roads can be taken: development induces anisotropic accessibility in morphospace. *Evol. Dev*. **16**, 373–381. (doi:10.1111/ede.12098)
49. Alexander RM. 2003 Modelling approaches in biomechanics. *Phil. Trans. R. Soc. Lond. B* **358**, 1429–1435. (doi:10.1098/rstb.2003.1336)
50. Zeffer A, Johansson CL, Marmebro A. 2003 Functional correlation between habitat use and leg morphology in birds (Aves). *Biol. J. Linn. Soc*. **79**, 461–484. (doi:10.1046/j.1095-8312.2003.00200.x)
51. Swartz SM, Bennett MB, Carrier DR. 1992 Wing bone stresses in free flying bats and the evolution of skeletal design for flight. *Nature* **359**, 726–729. (doi:10.1038/359726a0)
52. Palmer C, Dyke G. 2012 Constraints on the wing morphology of pterosaurs. *Proc. R. Soc. B* **279**, 1218–1224. (doi:10.1098/rspb.2011.1529)
53. Koob T, Long J. 2000 The vertebrate body axis: evolution and mechanical function. *Am. Zool*. **40**, 1–18. (doi:10.1668/0003-1569(2000)040[0001:TVBAEA]2.0.CO;2)
54. Habib M. 2010 The structural mechanics and evolution of aquaflying birds. *Biol. J. Linn. Soc*. **99**, 687–698. (doi:10.1111/j.1095-8312.2010.01372.x)
55. Archie JW. 1996 Measures of homoplasy. In *Homoplasy: the recurrence of similarity in evolution* (eds MJ Sanderson, L Hufford), pp. 153–188. Waltham, MA: Academic Press.
56. Archie JW. 1989 Homoplasy excess ratios: new indices for measuring levels of homoplasy in phylogenetic systematics and a critique of the consistency index. *Syst. Biol*. **38**, 253–269. (doi:10.2307/2992286)
57. Hoyal Cuthill J. 2015 The size of the character state space affects the occurrence and detection of homoplasy: modelling the probability of incompatibility for unordered phylogenetic characters. *J. Theor. Biol*. **366**, 24–32. (doi:10.1016/j.jtbi.2014.10.033)
58. Wagner PJ. 2000 Exhaustion of morphologic character states among fossil taxa. *Evolution* **54**, 365–386. (doi:10.1111/j.0014-3820.2000.tb00040.x)
59. Wagner PJ, Ruta M, Coates MI. 2006 Evolutionary patterns in early tetrapods. II. Differing constraints on available character space among clades. *Proc. R. Soc. B* **273**, 2113–2118. (doi:10.1098/rspb.2006.3561)
60. Ruta M, Wagner PJ, Coates MI. 2006 Evolutionary patterns in early tetrapods. I. Rapid initial diversification followed by decrease in rates of character change. *Proc. R. Soc. B* **273**, 2107–2111. (doi:10.1098/rspb.2006.3577)
61. R Development Core Team 2008 *R: A language and environment for statistical computing*. Vienna, Austria: R Foundation for Statistical Computing. (http://www.R-project.org)
62. Cailliez F. 1983 The analytical solution of the additive constant problem. *Psychometrika* **48**, 305–308. (doi:10.1007/BF02294026)
63. Gradstein FM, Ogg JG, Smith AG. 2004 *A geologic time scale*. Cambridge, UK: Cambridge University Press.
64. Ogg JG, Ogg G, Gradstein FM. 2008 *The concise geologic time scale*. Cambridge, UK: Cambridge University Press.
65. Sepkoski JJ. 2002 A compendium of fossil marine genera. *Bull. Am. Paleontol*. **363**, 1–563.
66. Benton MJ. 1993 *The fossil record 2*. London, UK: Chapman & Hall.
67. Alroy J. 2013 Fossilworks. www.fossilworks.org (accessed June 2015).
68. Uhen M. 1996 An evaluation of clade-shape statistics using simulations and extinct families of mammals. *Paleobiology* **22**, 8–22.
69. Huang S, Roy K, Jablonski D. 2015 Origins, bottlenecks, and present-day diversity: patterns of morphospace occupation in marine bivalves. *Evolution* **69**, 735–746. (doi:10.1111/evo.12608)
70. Goloboff P, Farris J, Nixon K. 2008 TNT, a free program for phylogenetic analysis. *Cladistics* **24**, 1–13. (doi:10.1111/j.1096-0031.2007.00173.x)
71. Fitch WM. 1971 Toward defining the course of evolution: minimum change for a specific tree topology. *Syst. Biol*. **20**, 406–416. (doi:10.1093/sysbio/20.4.406)
72. Wagner P, Sidor C. 2000 Age rank/clade rank metrics-sampling, taxonomy, and the meaning of 'stratigraphic consistency'. *Syst. Biol*. **49**, 463–479. (doi:10.1080/10635159950127349)
73. Lewis PO. 2001 A likelihood approach to estimating phylogeny from discrete morphological character data. *Syst. Biol*. **50**, 913–925. (doi:10.1080/10635150175346287 6)
74. Ronquist F, Huelsenbeck JP. 2003 MrBayes 3: Bayesian phylogenetic inference under mixed models. *Bioinformatics* **19**, 1572–1574. (doi:10.1093/bioinformatics/btg180)
75. Nylander JAA, Ronquist F, Huelsenbeck JP, Nieves-Aldrey JL. 2004 Bayesian phylogenetic analysis of combined data. *Syst. Biol*. **53**, 47–67. (doi:10.1080/10635150490264699)
76. Lloyd GT, Wang SC, Brusatte SL. 2012 Identifying heterogeneity in rates of morphological evolution: discrete character change in the evolution of lungfish (Sarcopterygii; Dipnoi). *Evolution* (*NY*). **66**, 330–348. (doi:10.5061/dryad.pg46f)
77. Bapst DW. 2014 Assessing the effect of time-scaling methods on phylogeny-based analyses in the fossil record. *Paleobiology* **40**, 331–351. (doi:10.1666/13033)
78. Dowd J, Riggs D. 1965 A comparison of estimates of Michaelis–Menten kinetic constants from various linear transformations. *J. Biol. Chem*. **240**, 863–869.
79. Hsu S, Hwang T, Kuang Y. 2001 Global analysis of the Michaelis–Menten-type ratio-dependent predator-prey system. *J. Math. Biol*. **42**, 489–506. (doi:10.1007/s002850100079)
80. Jorge Soberon M, Jorge Llorente B. 1993 The use of species accumulation functions for the prediction of species richness. *Conserv. Biol*. **7**, 480–488. (doi:10.1046/j.1523-1739.1993.07030480.x)
81. Anderson PSL, Friedman M, Brazeau MD, Rayfield EJ. 2011 Initial radiation of jaws demonstrated stability despite faunal and environmental change. *Nature* **476**, 206–209. (doi:10.1038/nature10207)
82. Sigurdsen T, Bolt JR. 2010 (Temnospondyli: Dissorophoidea), the interrelationships of amphibamids, and the origin of modern amphibians. *J. Vertebr. Paleontol*. **30**, 1360–1377. (doi:10.1080/02724634.2010.501445)
83. Hill J, Davis KE. 2014 The Supertree Toolkit 2: a new and improved software package with a Graphical User Interface for supertree construction. *Biodivers. Data J*. **2**, e1053. (doi:10.3897/BDJ.2.e1053)
84. Fröbisch J. 2007 The cranial anatomy of *Kombuisia frerensis* Hotton (Synapsida, Dicynodontia) and a new phylogeny of anomodont therapsids. *Zool. J. Linn. Soc*. **150**, 117–144. (doi:10.1111/j.1096-3642.2007.00285.x)
85. Hopkins SSB. 2008 Phylogeny and evolutionary history of the Aplodontoidea (Mammalia: Rodentia). *Zool. J. Linn. Soc*. **153**, 769–838. (doi:10.1111/j.1096-3642.2008.00399.x)
86. Dupret V, Zhu M, Wang JQ. 2009 The morphology of *Yujiangolepis liujingensis* (Placodermi, Arthrodira)

from the Pragian of Guangxi (south China) and its phylogenetic significance. *Zool. J. Linn. Soc.* **157**, 70–82. (doi:10.1111/j.1096-3642.2009.00519.x)

87. Fortey RA, Chatterton BDE. 1988 Classification of the trilobite suborder Asaphina. *Palaeontology* **31**, 165–222.
88. Lieberman BS, Kloc GJ. 1997 Evolutionary and biogeographic patterns in the Asteropyginae (Trilobita, Devonian) Delo, 1935. *Bull. Am. Museum Nat. Hist.* **232**.
89. Alvarez F, Jia-Yu R, Boucot AJ. 1998 The classification of athyridid brachiopods. *J. Paleontol.* **72**, 827–855.
90. Milner AC, Milner AR, Walsh SA. 2009 A new specimen of Baphetes from Nyrany, Czech Republic and the intrinsic relationships of the Baphetidae. *Acta Zool.* **90**, 318–334. (doi:10.1111/j.1463-6395.2008.00340.x)
91. Benedetto JL. 2009 Chaniella, a new lower Tremadocian (Ordovician) brachiopod from northwestern Argentina and its phylogenetic relationships within basal rhynchonelliforms. *Palaontologische Zeitschrift* **83**, 393–405. (doi:10.1007/s12542-009-0023-7)
92. Bodenbender BE, Fisher DC. 2001 Stratocladistic analysis of blastoid phylogeny. *J. Paleontol.* **75**, 351–369. (doi:10.1666/0022-3360(2001)075<0351:SAOBP>2.0.CO;2)
93. Foote M. 1992 Paleozoic record of morphological diversity in blastozoan echinoderms. *Proc. Natl Acad. Sci. USA* **89**, 7325–7329. (doi:10.1073/pnas.89.16.7325)
94. Wang X, Tedford RH, Taylor BE. 1999 Phylogenetic systematics of the Borophaginae (Carnivora, Canidae). *Bull. Am. Museum Nat. Hist.* **243**.
95. Gaffney ES, Tong H, Meylan PA. 2006 Evolution of the side-necked turtles: The families Bothremydidae, Euraxemydidae, and Araripemydidae. *Bull. Am. Museum Nat. Hist.* **300**.
96. Schoch RR, Milner AR. 2008 The intrarelationships and evolutionary history of the temnospondyl family Branchiosauridae. *J. Syst. Palaeontol.* **6**, 409–431. (doi:10.1017/S1477201908002460)
97. Mihlbachler M, Deméré TA. 2010 Phylogenetic status of Metarhinus pater (Brontotheriidae: Perissodactyla) from Southern California and species variation in Metarhinus from the middle Eocene of North America. *J. Vertebr. Paleontol.* **30**, 1229–1244. (doi:10.1080/02724634.2010.483568)
98. Jiménez-Sánchez A, Anstey RL, Azanza B. 2010 Description and phylogenetic analysis of *Iberostomata fombuenensis* new genus and species (Bryozoa, Ptilodictyina). *J. Paleontol.* **84**, 695–708. (doi:10.1666/09-068.1)
99. Sampson SD, Loewen MA, Farke AA, Roberts EM, Forster CA, Smith JA, Titus AL. 2010 New horned dinosaurs from Utah provide evidence for intracontinental dinosaur endemism. *PLoS ONE* **5**, 1–12. (doi:10.1371/journal.pone.0012292)
100. Smith AB, Zamora S. 2009 Rooting phylogenies of problematic fossil taxa; a case study using cinctans (stem-group echinoderms). *Palaeontology* **52**, 803–821. (doi:10.1111/j.1475-4983.2009.00880.x)
101. Carlson SJ, Fitzgerald PC. 2007 Sampling taxa, estimating phylogeny and inferring macroevolution: an example from Devonian terebratulide brachiopods. *Earth Environ. Sci. Trans. R. Soc. Edinburgh* **98**, 311–325. (doi:10.1017/S1755691007078437)
102. Novas FE, Pol D, Canale JI, Porfiri JD, Calvo JO. 2009 A bizarre Cretaceous theropod dinosaur from Patagonia and the evolution of Gondwanan dromaeosaurids. *Proc. Biol. Sci.* **276**, 1101–1107. (doi:10.1098/rspb.2008.1554)
103. Wenwei Y, Fortey RA, Turvey ST. 2006 Ontogeny and relationships of the trilobite *Pseudopetigurus* prantl and přibyl. *Palaeontology* **49**, 537–546. (doi:10.1111/j.1475-4983.2006.00546.x)
104. Clement AM, Long JA. 2010 Xeradipterus hatcheri, a new dipnoan from the Late Devonian (Frasnian) Gogo Formation, Western Australia, and other new holodontid material. *J. Vertebr. Paleontol.* **30**, 681–695. (doi:10.1080/02724631003763482)
105. Foote M. 1999 Morphological diversity in the evolutionary radiation of Paleozoic and post-Paleozoic crinoids. *Paleobiology* **25**, 1–115. (doi:10.2307/2666042)
106. Cotton JA, Fortey RA. 2005 Comparative morphology and relationships of the Agnostida. In *Crustacea and Arthropod Relationships* (eds S Koenemann, RA Jenner), pp. 95–136. Boca Raton, FL: CRC Press.
107. Maletz J, Carlucci J, Mitchell CE. 2009 Graptoloid cladistics, taxonomy and phylogeny. *Bull. Geosci.* **84**, 7–19. (doi:10.3140/bull.geosci.1108)
108. Bloch JI, Silcox MT, Boyer DM, Sargis EJ. 2007 New Paleocene skeletons and the relationship of plesiadapiforms to crown-clade primates. *Proc. Natl Acad. Sci. USA* **104**, 1159–1164. (doi:10.1073/pnas.0610579104)
109. Tetlie OE, Cuggy MB. 2007 Phylogeny of the basal swimming eurypterids (Chelicerata; Eurypterida; Eurypterina). *J. Syst. Palaeontol.* **5**, 345–356. (doi:10.1017/S1477201907002131)
110. Zhu M, Gai Z. 2007 Phylogenetic relationships of galeaspids (Agnatha). *Front. Biol. China* **2**, 151–169. (doi:10.1007/s11515-007-0022-6)
111. Korn D. 1997 Evolution of the Goniatitaceae and Viséan-Namurian biogeography. *Acta Palaeontol. Pol.* **42**, 177–199.
112. Gebauer EVl. 2007 Phylogeny and evolution of the Gorgonopsia with a special reference to the skull and skeleton of GPIT/RE/7113 ('Aelurognathus?' parringtoni). Dr. sc. nat. thesis, Geowissenschaften Fakultät, Eberhard Karls Universität Tübingen, Germany.
113. Prieto-Márquez A. 2010 Global phylogeny of hadrosauridae (Dinosauria: Ornithopoda) using parsimony and Bayesian methods. *Zool. J. Linn. Soc.* **159**, 435–502. (doi:10.1111/j.1096-3642.2009.00617.x)
114. Wang X. 1994 Phylogenetic systematics of the Hesperocyoninae (Carnivora: Canidae). *Bull. Am. Museum Nat. Hist.* **221**.
115. Polly PD. 1996 The skeleton of Gazinocyon vulpeculus gen. et comb. nov. and the cladistic relationships of Hyaenodontidae (Eutheria, Mammalia). *J. Vertebr. Paleontol.* **16**, 303–319. (doi:10.1080/02724634.1996.10011318)
116. Motani R. 1999 Phylogeny of the Ichthyopterygia. *J. Vertebr. Paleontol.* **19**, 473–496. (doi:10.1080/02724634.1999.10011160)
117. Trinajstic K, Dennis-Bryan K. 2009 Phenotypic plasticity, polymorphism and phylogeny within placoderms. *Acta Zool.* **90**, 83–102. (doi:10.1111/j.1463-6395.2008.00363.x)
118. Sundberg FA. 2004 Cladistic analysis of Early–Middle Cambrian kochaspid trilobites (Ptychopariida). *J. Paleontol.* **78**, 920–940. (doi:10.1666/0022-3360(2004)078<0920:CAOECK>2.0.CO;2)
119. Adrain JM, Chatterton BDE, Kloc G. 2008 Systematics of the koneprusiine trilobites, with new taxa from the Silurian and Devonian of Laurentia. *J. Paleontol.* **82**, 657–675.
120. Klembara J, Clack JA, Čerňanský A. 2010 The anatomy of palate of *Chroniosaurus dongusensis* (Chroniosuchia, Chroniosuchidae) from the Upper Permian of Russia. *Palaeontology* **53**, 1147–1153. (doi:10.1111/j.1475-4983.2010.00999.x)
121. Anderson JS, Reisz RR, Scott D, Fröbisch NB, Sumida SS. 2008 A stem batrachian from the Early Permian of Texas and the origin of frogs and salamanders. *Nature* **453**, 515–518. (doi:10.1038/nature06865)
122. Pollitt JR, Fortey RA, Wills MA. 2005 Systematics of the trilobite families Lichidae Hawle & Corda, 1847 and Lichakephalidae Tripp, 1957: The application of bayesian inference to morphological data. *J. Syst. Palaeontol.* **3**, 225–241. (doi:10.1017/S1477201905001604)
123. Yates A, Warren A. 2000 The phylogeny of 'higher' temnospondyls (Vertebrata: Choanata) and its implications for the monophyly and origins of the Stereospondyli. *Zool. J. Linn. Soc.* **128**, 77–121. (doi:10.1006/zjls)
124. Hoffmann R. 2010 New insights on the phylogeny of the Lytoceratoidea (Ammonitina) from the septal lobe and its functional interpretation. *Rev. Paleobiol.* **29**, 1–156.
125. Damiani RJ. 2001 A systematic revision and phylogenetic analysis of Triassic mastodonsauroids (Temnospondyli: Stereospondyli). *Zool. J. Linn. Soc.* **133**, 379–482. (doi:10.1006/zjls.2001.0304)
126. Young MT, De Andrade MB. 2009 What is Geosaurus? Redescription of *Geosaurus giganteus* (Thalattosuchia: Metriorhynchidae) from the Upper Jurassic of Bayern, Germany. *Zool. J. Linn. Soc.* **157**, 551–585. (doi:10.1111/j.1096-3642.2009.00536.x)
127. Polly PD, Wesley-Hunt GD, Heinrich RE, Davis GR, Houde P. 2006 Earliest known carnivoran auditory bulla and support for a recent origin of crown-group Carnivora (eutheria, mammalia). *Palaeontology* **49**, 1019–1027. (doi:10.1111/j.1475-4983.2006.00586.x)
128. Ruta M, Coates MI. 2007 Dates, nodes and character conflict: addressing the Lissamphibian origin problem. *J. Syst. Palaeontol.* **5**, 69–122. (doi:10.1017/S1477201906002008)
129. Lee SB, Lee DC, Choi DK. 2008 Cambrian-Ordovician trilobite family Missisquoiidae Hupé, 1955:

Systematic revision and palaeogeographical considerations based on cladistic analysis. *Palaeogeogr. Palaeoclimatol. Palaeoecol*. **260**, 315–341. (doi:10.1016/j.palaeo.2007.11.008)

130. Bell JL, Polcyn MJ. 2005 Dallasaurus turneri, a new primitive mosasauroid from the Middle Turonian of Texas and comments on the phylogeny of Mosasauridae (Squamata). *Netherlands J. Geosci. Geol. en Mijnb*. **84**, 177–194.
131. Kielan-Jaworowska Z, Hurum JH. 2001 Phylogeny and systematics of multituberculate mammals. *Palaeontology* **44**, 389–429. (doi:10.1111/1475-4983.00185)
132. Pol D, Leardi JM, Lecuona A, Krause M. 2012 Postcranial anatomy of *Sebecus icaeorhinus* (Crocodyliformes, Sebecidae) from the Eocene of Patagonia. *J. Vertebr. Paleontol*. **32**, 328–354. (doi:10.1080/02724634.2012.646833)
133. Lieberman BS. 2001 Phylogenetic analysis of the Olenellina Walcott, 1890 (Trilobita, Cambrian). *J. Paleontol*. **75**, 96–115. (doi:10.1666/0022-3360(2001)075<0096:PAOTOW>2.0.CO;2)
134. Lieberman BS. 1998 Cladistic analysis of the Early Cambrian Olenelloid trilobites. *J. Paleontol*. **72**, 59–78.
135. Bajpai S, Kay RF, Williams BA, Das DP, Kapur VV, Tiwari BN. 2008 The oldest Asian record of Anthropoidea. *Proc. Natl Acad. Sci. USA* **105**, 11 093–11 098. (doi:10.1073/pnas.0804159105)
136. McDonald AT, Kirkland JI, DeBlieux DD. 2010 New basal iguanodonts from the Cedar Mountain Formation of Utah and the evolution of thumb-spiked dinosaurs. *PLoS ONE* **5**, e14075. (doi:10.1371/journal.pone.0014075)
137. Mitchell CE. 1987 Evolution and phylogenetic classification of the Diplograptacea. *Palaeontology* **30**, 353–405.
138. Sansom RS. 2009 Phylogeny, classification and character polarity of the Osteostraci (Vertebrata). *J. Syst. Palaeontol*. **7**, 95–115. (doi:10.1017/S1477201908002551)
139. Longrich NR, Sankey J, Tanke D. 2010 Texacephale langstoni, a new genus of pachycephalosaurid (Dinosauria: Ornithischia) from the upper Campanian Aguja Formation, southern Texas, USA. *Cretac. Res*. **31**, 274–284. (doi:10.1016/j.cretres.2009.12.002)
140. Prokop J, Ren D. 2007 New significant fossil insects from the Upper Carboniferous of Ningxia in northern China (Palaeodictyoptera, Archaeorthoptera). *Eur. J. Entomol*. **104**, 267–275.
141. Jin J, Popov LE. 2008 A new genus of Late Ordovician—Early Silurian Pentameride brachiopods and its phylogenetic relationships. *Acta Palaeontol. Pol*. **53**, 221–236. (doi:10.4202/app.2008.0205)
142. Stocker MR. 2010 A new taxon of phytosaur (Archosauria: Pseudosuchia) from the Late Triassic (Norian) Sonsela Member (Chinle Formation) in Arizona, and a critical reevaluation of Leptosuchus Case, 1922. *Palaeontology* **53**, 997–1022. (doi:10.1111/j.1475-4983.2010.00983.x)
143. López-Arbarello A, Zavattieri AM. 2008 Systematic revision of Pseudobeaconia Bordas, 1944, and Mendocinichthys Whitley, 1953 (Actinopterygii: 'Perleidiformes') from the Triassic of Argentina. *Palaeontology* **51**, 1025–1052. (doi:10.1111/j.1475-4983.2008.00806.x)
144. Smith ND, Pol D. 2007 Anatomy of a basal sauropodomorph dinosaur from the Early Jurassic Hanson Formation of Antarctica. *Acta Palaeontol. Pol*. **52**, 657–674.
145. Ketchum HF, Benson RBJ. 2010 Global interrelationships of Plesiosauria (Reptilia, Sauropterygia) and the pivotal role of taxon sampling in determining the outcome of phylogenetic analyses. *Biol. Rev*. **85**, 361–392. (doi:10.1111/j.1469-185X.2009.00107.x)
146. Smith AS, Dyke GJ. 2008 The skull of the giant predatory pliosaur Rhomaleosaurus cramptoni: implications for plesiosaur phylogenetics. *Naturwissenschaften* **95**, 975–980. (doi:10.1007/s00114-008-0402-z)
147. Cisneros JC, Ruta M. 2010 Morphological diversity and biogeography of procolophonids (Amniota: Parareptilia). *J. Syst. Palaeontol*. **8**, 607–625. (doi:10.1080/14772019.2010.491986)
148. Huguet A, Nel A, Martinez-Delclos X, Bechly G. 2002 Preliminary phylogenetic analysis of the Protanisoptera (Insecta: Odonatoptera). *Geobios* **35**, 537–560.
149. Nel A, Petrulevicius JF, Martínez-Delclós X. 2005 New mesozoic protomyrmeleontidae (Insecta: Odonatoptera: Archizygoptera) from Asia with a new phylogenetic analysis. *J. Syst. Palaeontol*. **3**, 187–201. (doi:10.1017/S1477201905001549)
150. Egi N, Holroyd PA, Tsubamoto T, Soe AN, Takai M, Ciochon RL. 2005 Proviverrine hyaenodontids (Creodonta: Mammalia) from the Eocene of Myanmar and a phylogenetic analysis of the proviverrines from the Para-Tethys area. *J. Syst. Palaeontol*. **3**, 337–358. (doi:10.1017/S1477201905001707)
151. Parker W, Irmis R. 2006 A new species of the Late Triassic phytosaur Pseudopalatus (Archosauria: Pseudosuchia) from Petrified Forest National Park, Arizona. *Museum North. Arizona Bull*. **295**, 160–161. (doi:10.1098/rspb.2005.3426.Fisher)
152. Pernègre VN, Elliott DK. 2008 Phylogeny of the Pteraspidiformes (Heterostraci), Silurian-Devonian jawless vertebrates. *Zool. Scr*. **37**, 391–403. (doi:10.1111/j.1463-6409.2008.00333.x)
153. Lü J, Unwin DM, Jin X, Liu Y, Ji Q. 2010 Evidence for modular evolution in a long-tailed pterosaur with a pterodactyloid skull. *Proc. Biol. Sci*. **277**, 383–389. (doi:10.1098/rspb.2009.1603)
154. Poyato Ariza FJ, Wenz S. 2002 A new insight into pycnodontiform fishes. *Geodiversitas* **24**, 139–248.
155. Brusatte SL, Benton MJ, Desojo JB, Langer MC. 2010 The higher-level phylogeny of Archosauria (Tetrapoda: Diapsida). *J. Syst. Palaeontol*. **8**, 3–47. (doi:10.1080/14772010903537732)
156. Bates DEB, Kozlowska A, Lenz AC. 2005 Silurian retiolitid graptolites: morphology and evolution. *Acta Palaeontol. Pol*. **50**, 705–720.
157. Cerdeno E. 1995 Cladistic analysis of the family Rhinocerotidae (Perissodactyla). *Am. Museum Novit*. **3143**.
158. Hone DWE, Benton MJ. 2008 A new genus of rhynchosaur from the Middle Triassic of South-west England. *Palaeontology* **51**, 95–115. (doi:10.1111/j.1475-4983.2007.00739.x)
159. Allain R, Aquesbi N. 2008 Anatomy and phylogenetic relationships of *Tazoudasaurus naimi* (Dinosauria, Sauropoda) from the late Early Jurassic of Morocco. *Geodiversitas* **30**, 345–424. (doi:10.1080/08912960903562317)
160. Maidment SCR. 2010 Stegosauria: a historical review of the body fossil record and phylogenetic relationships. *Swiss J. Geosci*. **103**, 199–210. (doi:10.1007/s00015-010-0023-3)
161. Schoch RR. 2008 A new stereospondyl from the German Middle Triassic, and the origin of the Metoposauridae. *Zool. J. Linn. Soc*. **152**, 79–113. (doi:10.1111/j.1096-3642.2007.00363.x)
162. Lamsdell JC, Braddy SJ, Tetlie OE. 2010 The systematics and phylogeny of the Stylonurina (Arthropoda: Chelicerata: Eurypterida). *J. Syst. Palaeontol*. **8**, 49–61. (doi:10.1080/14772011003603564)
163. Klug S. 2010 Monophyly, phylogeny and systematic position of the synechodontiformes (Chondrichthyes, Neoselachii). *Zool. Scr*. **39**, 37–49. (doi:10.1111/j.1463-6409.2009.00399.x)
164. Gaudin TJ. 2004 Phylogenetic relationships among sloths (Mammalia, Xenarthra, Tardigrada): the craniodental evidence. *Zool. J. Linn. Soc*. **140**, 255–305. (doi:10.1111/j.1096-3642.2003.00100.x)
165. Wu X-C, Cheng Y-N, Sato T, Shan H-Y. 2009 Miodentosaurus brevis Cheng *et al.*, 2007 (Diapsida: Thalattosauria): its postcranial skeleton and phylogenetic relationships. *Vertebr. Palasiat*. **47**, 1–20.
166. Wilson MV, Märss T. 2009 Thelodont phylogeny revisited, with inclusion of key scale-based taxa. *Est. J. Earth Sci*. **58**, 297. (doi:10.3176/earth.2009.4.08)
167. Hu D, Hou L, Zhang L, Xu X. 2009 A pre-Archaeopteryx troodontid theropod from China with long feathers on the metatarsus. *Nature* **461**, 640–643. (doi:10.1038/nature08322)
168. Chatterton BDE, Edgecombe GD, Waisfeld BG, Vaccari NE. 1998 Ontogeny and systematics of Toernquistiidae (trilobita, proetida) from the ordovician of the Argentine Precordillera. *J. Paleontol*. **72**, 273–303.
169. Brusatte SL, *et al.* 2010 Tyrannosaur paleobiology: new research on ancient exemplar organisms. *Science* **329**, 1481–1485. (doi:10.1126/science.1193304)
170. Anderson LI, Selden PA. 1997 Opisthosomal fusion and phylogeny of Palaeozoic Xiphosura. *Lethaia* **30**, 19–31. (doi:10.1111/j.1502-3931.1997.tb00440.x)
171. Mitchell CE. 1987 Evolution and phylogenetic classification of the Diplograptacea. *Palaeontology* **30**, 353–405.
172. Fortey RRA, Chatterton BDE. 1988 Classification of the trilobite suborder: Asaphina. *Palaeontology* **31**, 165–222.
173. Smith AB, Zamora S. 2009 Rooting phylogenies of problematic fossil taxa; a case study using cinctans

(stem-group echinoderms). *Palaeontology* **52**, 803–821. (doi:10.1111/j.1475-4983.2009.00880.x)
174. Gaffney ES, Tong H, Meylan PA. 2006 Evolution of the side-necked turtles: the families Bothremydidae, Euraxemydidae, and Araripemydidae. *Bull. Am. Museum Nat. Hist*. **300**, 1–698. (doi:10.1206/0003-0090(2006)300[1:EOTSTT]2.0.CO;2)
175. Ketchum HF, Benson RBJ. 2010 Global interrelationships of Plesiosauria (Reptilia, Sauropterygia) and the pivotal role of taxon sampling in determining the outcome of phylogenetic analyses. *Biol. Rev. Camb. Philos. Soc*. **85**, 361–392. (doi:10.1111/j.1469-185X.2009.00107.x)
176. Hopkins SSB. 2008 Phylogeny and evolutionary history of the Aplodontoidea (Mammalia: Rodentia). *Zool. J. Linn. Soc*. **153**, 769–838. (doi:10.1111/j.1096-3642.2008.00399.x)
177. Hopkins MJ, Smith AB. 2015 Dynamic evolutionary change in post-Paleozoic echinoids and the importance of scale when interpreting changes in rates of evolution. *Proc. Natl Acad. Sci. USA* **112**, 3758–3763. (doi:10.1073/pnas.1418153112)
178. Galis F, Metz JAJ. 2007 Evolutionary novelties: the making and breaking of pleiotropic constraints. *Integr. Comp. Biol*. **47**, 409–419. (doi:10.1093/icb/icm081)
179. Salinas-Saavedra M, Gonzalez-Cabrera C, Ossa-Fuentes L, Botelho JF, Ruiz-Flores M, Vargas AO. 2014 New developmental evidence supports a homeotic frameshift of digit identity in the evolution of the bird wing. *Front. Zool*. **11**, 33. (doi:10.1186/1742-9994-11-33)
180. Wills MA. 1998 Cambrian and recent disparity: the picture from priapulids. *Paleobiology* **24**, 177–199.
181. Wills MA, Gerber S, Ruta M, Hughes M. 2012 The disparity of priapulid, archaeopriapulid and palaeoscolecid worms in the light of new data. *J. Evol. Biol*. **25**, 2056–2076. (doi:10.1111/j.1420-9101.2012.02586.x)
182. Gerber S. 2011 Comparing the differential filling of morphospace and allometric space through time: the morphological and developmental dynamics of Early Jurassic ammonoids. *Paleobiology* **37**, 369–382. (doi:10.1666/10005.1)
183. Brakefield PM. 2008 Prospects of evo-devo for linking pattern and process in the evolution of morphospace. In *Evolving pathways: key themes in evolutionary developmental biology* (eds A Minelli, G Fusco), pp. 62–79. Cambridge, UK: Cambridge University Press.
184. Mitteroecker P, Huttegger SM. 2009 The concept of morphospaces in evolutionary and developmental biology: mathematics and metaphors. *Biol. Theory* **4**, 54–67. (doi:10.1162/biot.2009.4.1.54)
185. Gerber S, Eble G, Neige P. 2011 Developmental aspects of morphological disparity dynamics: a simple analytical exploration. *Paleobiology* **37**, 237–251. (doi:10.1111/j.1558-5646.2008.00370.x)
186. Young NM *et al.* 2014 Embryonic bauplans and the developmental origins of facial diversity and constraint. *Development* **141**, 1059–1063. (doi:10.1242/dev.099994)
187. Goswami A, Polly PD. 2010 The influence of modularity on cranial morphological disparity in Carnivora and primates (mammalia). *PLoS ONE* **5**, e9517. (doi:10.1371/journal.pone.0009517)
188. Anderson LC, Roopnarine PD. 2005 Role of constraint and selection in the morphologic evolution of Caryocorbula (Mollusca: Corbulidae) from the Caribbean Neogene. *Palaeontol. Electron*. **8**, 1–18.
189. Young CC, Zhao X-J. 1972 *Mamenchisaurus hochuanensis* sp. nov. *Inst. Vertebr. Paleontol. Paleoanthropology Monogr*. **8**, 1–30.
190. Sachs S, Kear BP, Everhart MJ. 2013 Revised vertebral count in the 'longest-necked vertebrate' *Elasmosaurus platyurus* Cope 1868, and clarification of the cervical-dorsal transition in Plesiosauria. *PLoS ONE* **8**, e70877. (doi:10.1371/journal.pone.0070877)
191. Varela-Lasheras I, Bakker AJ, van der Mije SD, Metz JAJ, van Alphen J, Galis F. 2011 Breaking evolutionary and pleiotropic constraints in mammals: on sloths, manatees and homeotic mutations. *Evodevo* **2**, 1–27. (doi:10.1186/2041-9139-2-11)
192. Galis F. 1999 Why do almost all mammals have seven cervical vertebrae? Developmental constraints, *Hox* genes, and cancer. *J. Exp. Zool*. **285**, 19–26. (doi:10.1073/(SICI)1097-010X(19990415)285:1<19::AID-JEZ3>3.0.CO;2-Z)
193. Galis F, Metz JAJ. 2003 Anti-cancer selection as a source of developmental and evolutionary constraints. *Bioessays* **25**, 1035–1039. (doi:10.1002/bies.10366)
194. Galis F, van Alphen JJM, Metz JAJ. 2001 Why five fingers? Evolutionary constraints on digit numbers. *Trends Ecol. Evol*. **16**, 637–647. (doi:10.1016/S0169-5347(01)02289-3)
195. Mitgutsch C, Richardson MK, Jimenez R, Martin JE, Kondrashov P, de Bakker MAG, Sanchez-Villagra MR. 2012 Circumventing the polydactyly 'constraint': the mole's 'thumb.' *Biol. Lett*. **8**, 74–77. (doi:10.1098/rsbl.2011.0494)
196. Wu X-C, Li Z, Zhou B-C, Dong Z-M. 2003 A polydactylous amniote from the Triassic period. *Nature* **426**, 516. (doi:10.1038/426516a)
197. Motani R. 1999 On the evolution and homologies of ichthyopterygian forefins. *J. Vertebr. Paleontol*. **19**, 28–41. (doi:10.1080/02724634.1999.10011120)
198. Lande R. 1978 Evolutionary mechanisms of limb loss in tetrapods. *Evolution* (*N.Y*). **32**, 73–92.
199. Alberch P. 1985 Why St. Bernards often have an extra digit and poodles never do. *Am. Nat*. **126**, 430–433. (doi:10.2307/2678832)
200. Quinonez SC, Innis JW. 2014 Human *HOX* gene disorders. *Mol. Genet. Metab*. **111**, 4–15. (doi:10.1016/j.ymgme.2013.10.012)
201. Villier L, Korn D. 2004 Morphological disparity of ammonoids and the mark of Permian mass extinctions. *Science* (*80-*.). **306**, 264–266. (doi:10.1126/science.1102127)
202. Hopkins MJ. 2013 Decoupling of taxonomic diversity and morphological disparity during decline of the Cambrian trilobite family Pterocephaliidae. *J. Evol. Biol*. **26**, 1665–1676. (doi:10.1111/jeb.12164)
203. Luo Z-X. 2007 Transformation and diversification in early mammal evolution. *Nature* **450**, 1011–1019. (doi:10.1038/nature06277)
204. Ciampaglio CN. 2004 Measuring changes in articulate brachiopod morphology before and after the Permian mass extinction event: do developmental constraints limit morphological innovation? *Evol. Dev*. **6**, 260–274. (doi:10.1111/j.1525-142X.2004.04031.x)
205. Korn D, Hopkins MJ, Walton SA. 2013 Extinction space: a method for the quantification and classification of changes in morphospace across extinction boundaries. *Evolution* (*NY*). **67**, 2795–2810. (doi:10.1111/evo.12162)